Convergent origin and accelerated evolution of vesicle-associated RhoGAP proteins in two unrelated parasitoid wasps

Dominique Colinet*[1], Fanny Cavigliasso[1], Matthieu Leobold[2], Appoline Pichon[3], Serge Urbach[3], Dominique Cazes[1], Marine Poullet[1], Maya Belghazi[4], Anne-Nathalie Volkoff[3], Jean-Michel Drezen[2], Jean-Luc Gatti[1], and Marylène Poirié[1]

[1] Université Côte d'Azur, INRAE, CNRS, ISA, 06903 Sophia Antipolis, France
[2] Institut de Recherche sur la Biologie de l'Insecte (IRBI), UMR 7261, CNRS - Université de Tours, Tours, France
[3] DGIMI, Univ Montpellier, INRAE, 34095 Montpellier, France
[4] Aix Marseille Université, CNRS, Plateforme Protéomique, IMM FR3479, Marseille Protéomique (MaP), 13402 Marseille, France

*Corresponding author
Correspondence: dominique.colinet@inrae.fr

Abstract

Animal venoms and other protein-based secretions that perform a variety of functions, from predation to defense, are highly complex cocktails of bioactive compounds. Gene duplication, accompanied by modification of the expression and/or function of one of the duplicates under the action of positive selection, followed by further duplication to produce multigene families of toxins is a well-documented process in venomous animals. This evolutionary model has been less described in parasitoid wasps, which use maternal fluids, including venom, to protect their eggs from encapsulation by the host immune system. Here, we evidence the convergent recruitment and accelerated evolution of two multigene families of RhoGAPs presumably involved in virulence in two unrelated parasitoid wasp species, *Leptopilina boulardi* (Figitidae) and *Venturia canescens* (Icheumonidae). In both species, these RhoGAPs are associated with vesicles that act as transport systems to deliver virulence factors, but are produced in different tissues: the venom gland in *Leptopilina* sp. and the ovarian calyx in *V. canescens*. We show that the gene encoding the cellular RacGAP1 is at the origin of the virulent RhoGAP families found in *Leptopilina* sp. and *V. canescens*. We also show that both RhoGAP families have undergone evolution under positive selection and that almost all of these RhoGAPs lost their GAP activity and GTPase binding ability due to mutations in key amino acids. These results suggest an accelerated evolution and functional diversification of these vesicle-associated RhoGAPs in the two phylogenetically distant parasitoid species. The potential new function(s) and the exact mechanism of action of these proteins in host cells remain to be elucidated.

Keywords: parasitoids, venom and other secretions, RhoGAP multigene family, evolution, gene duplication, positive selection

Introduction

Gene duplication is recognized as an important evolutionary process because it drives functional novelty (Chen et al., 2013; Long et al., 2013). In particular, the formation of multigene families by repeated gene duplication is a widely studied evolutionary process in several groups of venomous animals (Fry et al., 2009; Wong & Belov 2012; Casewell et al., 2013), but also in some parasites (Akhter et al., 2012; Arisue et al., 2020). Such repeated duplication events of venomous or virulence protein-coding genes are often accompanied by significant copy divergence through positive selection, allowing the acquisition of new functions. In this work, we studied the process of accelerated evolution by duplication and divergence of two multigene families encoding RhoGAPs presumably involved in virulence in two phylogenetically distant parasitoid wasp species, *Leptopilina* species of the family Figitidae and *Venturia canescens* of the family Icheumonidae.

The development of parasitoid wasps occurs at the expense of another arthropod, whose tissues are consumed by the parasitoid larvae, usually resulting in the host death (Godfray 1994). For endoparasitoids that lay eggs inside the host body, the host immune defense against parasitoids is usually based on the formation of a multicellular melanized capsule around the parasitoid egg, resulting in its death (Carton et al., 2008). To escape encapsulation, parasitoids have evolved several strategies, the main one being the injection of maternal fluids together with the egg into the host at the time of oviposition (Pennacchio & Strand 2006; Poirié et al., 2009). These maternal fluids contain (i) proteins synthesized in the venom glands (Asgari & Rivers 2010; Poirié et al., 2014), some of which, as in *Leptopilina,* can be associated with extracellular vesicles called venosomes and allow their transport to the targeted immune cells (Gatti et al., 2012; Wan et al., 2019), (ii) proteins synthesized in the ovarian calyx cells and associated with particles of viral origin devoid of nucleic acid and named virus-like particles (VLPs) as in *V. canescens* (Reineke et al., 2006; Gatti et al., 2012; Pichon et al., 2015), and (iii) polydnaviruses (PDVs) integrated into the parasitoid genome and found in some groups of parasitoids belonging to the families Braconidae and Ichneumonidae (Drezen et al., 2014). Like VLPs, PDVs are synthesized in the ovarian calyx cells and are present in the ovarian fluid along with the egg. These particles are unique in that they are formed by the integrated viral machinery, but carry circular double-stranded DNA molecules that contain virulence genes that will be expressed in the host cells (Drezen et al., 2014). The process of accelerated evolution by duplication and divergence has been described for some of these virulence genes carried by PDVs, suggesting functional diversification of the proteins produced (Serbielle et al., 2008; Serbielle et al., 2012; Jancek et al., 2013).

Leptopilina boulardi is a parasitoid wasp of *Drosophila* for which two lines have been well characterized (Dubuffet et al., 2009). The ISm line of *L. boulardi* is highly virulent against *Drosophila melanogaster* but is unable to develop in *Drosophila yakuba* whereas the ISy line can develop in both *Drosophila* species but its success depends on the resistance/susceptibility of the host (Dubuffet et al., 2009). One of the most abundant proteins in the venom of the *L. boulardi* ISm line belongs to the Rho GTPase activating protein (RhoGAP) family and has been named LbGAP (Labrosse et al., 2005; Colinet et al., 2013). A LbGAP homolog named LbGAPy is also present in the venom of the *L. boulardi* ISy line, but in lower amounts (Colinet et al., 2010; Colinet et al., 2013). While RhoGAPs are usually intracellular proteins composed of several different domains (Tcherkezian & Lamarche-Vane 2007), LbGAP and LGAPy contain only one RhoGAP domain preceded by a signal peptide that allows its secretion. LbGAP has been shown to be associated with and transported by venosomes to target host hemocytes (Wan et al., 2019). LbGAP and LbGAPy specifically interact with and inactivate two *Drosophila* Rho GTPases, Rac1 and Rac2 (Colinet et al., 2007; Colinet et al., 2010), which are required for hemocyte proliferation in response to parasitism, hemocyte adhesion around the parasitoid egg, or the formation of intercellular junctions necessary for the capsule formation (Williams et al., 2005; Williams et al., 2006). Combined transcriptomic and proteomic analyses have identified eight additional RhoGAP domain-containing venom proteins in addition to LbGAP and LbGAPy for both *L. boulardi* lines, suggesting that a multigene family has derived from repeated duplication (Colinet et al., 2013). One of these venom RhoGAPs, LbGAP2, has also been shown to be associated with venosomes in *L. boulardi* ISm and to be released with LbGAP in host hemocytes (Wan et al., 2019). Interestingly, three RhoGAP domain-containing venom proteins have also been identified in the closely related species *Leptopilina heterotoma* (Colinet et al., 2013), suggesting that the recruitment of RhoGAPs in the venom arsenal may have occurred before the separation of the two species.

Leptopilina venom RhoGAPs are not the only example of the possible use of a protein from this family in parasitoid virulence (Reineke et al., 2006; Du et al., 2020). In the Ichneumonidae *V. canescens*, a RhoGAP domain-containing protein known as VLP2 (named VcVLP2 in this paper) was found to be associated with VLPs formed in the nucleus of ovarian calyx cells (Reineke et al., 2006; Pichon et al., 2015). VLPs, which package proteic virulence factors wrapped into viral envelopes, are then released into the ovarian lumen to associate with eggs and protect them from the host immune response by as yet unknown mechanisms (Feddersen et al., 1986). These observations suggest convergent recruitment of proteins belonging to the same family and injected into the host with the egg in two phylogenetically distant parasitoid species.

In this work, we showed that VcVLP2 in *V. canescens*, like LbGAP in *Leptopilina*, is not unique but is part of a multigene family of virulent RhoGAPs associated with extracellular vesicles. RhoGAPs from different organisms are grouped into distinct subfamilies based on similarities in RhoGAP domain sequence and overall multi-domain organization (Tcherkezian & Lamarche-Vane 2007). Our analyses indicate that an independent duplication of the RacGAP1 gene, a member of the large RhoGAP family, was the origin of the virulent RhoGAP multigene families found in *Leptopilina* and *V. canescens*. We then performed comparative analyses to understand the duplication events at the origin of these two multigene families. Finally, we demonstrated evolution under positive selection for both RhoGAP multigene families in *L. boulardi* and *V. canescens,* suggesting accelerated evolution and functional diversification.

Methods

Biological material

The origin of the *L. boulardi* isofemale lines ISm (Lbm; Gif stock number 431) and ISy (Lby; Gif stock number 486) has been described previously (Dupas et al., 1998). Briefly, the ISy and ISm founding females were collected in Brazzaville (Congo) and Nasrallah (Tunisia), respectively. The *L. heterotoma* strain (Lh; GIF stock number 548) was collected in southern France (Gotheron). The Japanese strain of *Leptopilina victoriae* (Lv), described in Novković et al., 2011, was provided by Pr. M. T. Kimura (Hokkaido University, Japan). All parasitoid lines were reared on a susceptible *D. melanogaster* Nasrallah strain (Gif stock number 1333) at 25 °C. After emergence, the wasps were maintained at 20 °C on agar medium supplemented with honey. All experiments were performed on 5- to 10-day-old parasitoid females.

Phylogeny of members of the Cynipoidea superfamily

The phylogeny of selected members of the Cynipoidea superfamily was constructed using internal transcribed spacer 2 (ITS2) sequences available at NCBI (Supplementary Table S1). Multiple sequence alignment was performed using MAFFT with the --auto option (Katoh & Standley 2013). Poorly aligned regions were removed using trimal with the -automated1 option (Capella-Gutierrez et al., 2009). Phylogenetic analysis was performed using maximum likelihood (ML) with IQ-TREE (Minh et al., 2020).

Search for candidate venom RhoGAPs in Leptopilina transcriptomes

L. victoriae venom apparatus, corresponding to venom glands and associated reservoirs, were dissected in Ringer's saline (KCl 182 mM; NaCl 46 mM; $CaCl_2$ 3 mM; Tris-HCl 10 mM). Total RNA was extracted from 100 venom apparatus using TRIzol reagent (Invitrogen) followed by RNeasy Plus Micro Kit (QIAGEN) according to the manufacturers' instructions. The quality of total RNA was checked using an Agilent BioAnalyzer. Illumina RNASeq sequencing (HiSeq 2000, 2 × 75 pb) and trimming were performed by Beckman Coulter Genomics. The raw data are available at NCBI under the BioProject ID PRJNA974978. Sequence assembly was performed using the "RNASeq de novo assembly and abundance estimation with Trinity and cdhit" workflow available on Galaxy at the BIPAA platform (https://bipaa.genouest.org).

Leptopilina clavipes (whole body), *Ganaspis* sp. G1 (female abdomen), *Andricus quercuscalicis* (whole body) and *Synergus umbraculus* (whole body) transcriptomes were obtained from NCBI under accession numbers GAXY00000000, GAIW00000000, GBNY00000000 and GBWA00000000, respectively. Coding regions in the transcripts were identified and translated using TransDecoder (Haas et al., 2013), which is available on the BIPAA Galaxy platform. Searches for RhoGAP domain-containing sequences in translated coding sequences were performed using hmmsearch from the HMMER package (Eddy 2009) with the RhoGAP (PF00620) HMM profile.

145 **Completion of *L. boulardi* and *L. heterotoma* venom RhoGAP sequences**
146 Venom apparatus, corresponding to venom glands and associated reservoirs, were dissected in Ringer's
147 saline. Total RNA was extracted from venom apparatus using the RNeasy Plus Micro Kit (QIAGEN) according
148 to the manufacturers' instructions. To obtain the full-length coding sequence of LbGAP1.3, LbGAP5,
149 LbGAPy6, LhGAP1 and LhGAP2, rapid amplification of cDNA ends (RACE) was performed using the SMART
150 RACE cDNA Amplification Kit (Clontech). For LhGAP3, 3' RACE could not be applied due to the presence of
151 poly(A) stretches in the sequence. LhGAP3-matching sequences were searched for in the transcriptome
152 assembly obtained by Goecks et al., 2013) from the abdomen of *L. heterotoma* females (GenBank accession
153 number GAJC00000000) using the command line NCBI-BLAST package (version 2.2.24). The resulting
154 complete LhGAP3 sequence was then verified by RT-PCR using the iScript cDNA Synthesis Kit (BioRad) and
155 the GoTaq DNA Polymerase (Promega), followed by direct sequencing of the amplified fragment. Geneious
156 software (Biomatters) was used for sequence editing and assembly.

157 **Obtention of Leptopilina RacGAP1 coding sequences**
158 A combination of RT-PCR and RACE using conserved and specific primers was used to clone the full-
159 length ORF sequence of *L. boulardi* and *L. heterotoma* RacGAP1. The amino acid sequence of *Nasonia*
160 *vitripennis* RacGAP1 (Supplementary Table S2) was used to search for similar sequences among
161 Hymenoptera species using BLASTP at NCBI (http://www.ncbi.nlm.nih.gov/blast/). A multiple sequence
162 alignment of the RacGAP1 amino acid sequences found in Hymenoptera was then performed using
163 MUSCLE (Edgar 2004). Two pairs of RacGAP1-specific degenerate primers were designed from the
164 identified conserved regions (Supplementary Figure S1). Total RNA was extracted from Lbm and Lh
165 individuals using the TRIzol reagent (Invitrogen), and RT-PCR experiments were performed using the
166 RacGAP1-specific degenerate primers. After direct sequencing of the amplified fragments, Lbm- and Lh-
167 specific primers were designed to complete the sequences obtained by RT-PCR and RACE (Supplementary
168 Figure S1). The coding sequences of *L. victoriae and L. clavipes* RacGAP1 were obtained by BLAST searches
169 in the corresponding transcriptomes using *L. boulardi* and *L. heterotoma* RacGAP1 sequences as queries.

170 **Obtention of the genomic sequences of Leptopilina venom RhoGAPs and RacGAP1**
171 The genomic sequences of *Leptopilina* venom RhoGAPs and RacGAP1 were obtained by BLAST and
172 Exonerate searches (Slater & Birney 2005) using the corresponding coding sequences as queries. *L. boulardi*
173 ISm, *L. boulardi* ISy, *L. heterotoma* and *L. clavipes* genome assemblies were obtained from NCBI under
174 accession numbers GCA_011634795.1, GCA_019393585.1, GCF_015476425.1 and GCA_001855655.1
175 respectively.

176 **Search for candidate *V. canescens* RhoGAP calyx sequences**
177 Coding regions were identified from the *V. canescens* calyx transcriptome published by Pichon et al.,
178 *(*2015) and translated into protein sequences using TransDecoder (Haas et al., 2013). The search for
179 RhoGAP domain-containing sequences was performed using hmmsearch from the HMMER package (Eddy
180 2009) with the RhoGAP (PF00620) HMM profile. The identified RhoGAP calyx sequences were used as a
181 database for Mascot to explore MS/MS data obtained from purified *V. canescens* VLPs (Pichon et al., 2015)
182 with a false discovery rate of 1%. Only proteins identified by two or more peptides were considered.
183 The *V. canescens* RacGAP1 coding sequence was obtained by BLAST searches in the *V. canescens* calyx
184 transcriptome using the *N. vitripennis* RacGAP1 sequence as query.
185 The *V. canescens* calyx RhoGAP and RacGAP1 genome sequences were obtained by BLAST and
186 Exonerate searches (Slater and Birney 2005) using the corresponding coding sequences as queries. The *V.*
187 *canescens* genome assembly was obtained from NCBI under accession number GCA_019457755.1.

188 **Identification of domains and motifs and prediction of subcellular localization**
189 The presence and position of signal peptide cleavage sites in the identified RhoGAP domain-containing
190 sequences were predicted using the SignalP server
191 (https://services.healthtech.dtu.dk/service.php?SignalP). The searches for domains and motifs were
192 performed using InterProScan 5 (Jones et al., 2014). Coiled-coil regions were predicted using COILS (Lucas
193 et al., 1991).

194 Prediction of protein subcellular localization and sorting signals for *Venturia* RacGAP1 and calyx
195 RhoGAPs was performed using the DeepLoc2 server (https://services.healthtech.dtu.dk/services/DeepLoc-
196 2.0/).
197 Nuclear localization for VcRacGAP1 and calyx RhoGAPs was also predicted using the following three
198 tools: NucPred (Brameier et al., 2007) was used to indicate whether a protein spends part of its time in the
199 nucleus (https://nucpred.bioinfo.se/nucpred/), LocTree3 (Goldberg et al., 2014) to provide subcellular
200 localization and Gene Ontology terms (https://rostlab.org/services/loctree3/), and PSORT II (Nakai &
201 Horton 1999) to detect sorting signals and subcellular localization (https://psort.hgc.jp/form2.html).
202 PSORT II results corresponding to ER membrane retention signals and cleavage sites for mitochondrial
203 presequences were included as they may be associated with nuclear localization. Mitochondrial
204 presequences have no sequence homology but possess physical characteristics that allow them to interact
205 with the outer membranes of mitochondria and thus allow the targeting of proteins to the mitochondrial
206 matrix. Regarding mitochondrial targeting, it has been shown from plants to humans that some proteins
207 with mitochondrial presequences are dually targeted to mitochondria and the nucleus (Millar et al., 2006;
208 Mueller et al., 2004). Indeed, anchoring signals to the ER membrane are known to allow baculoviral
209 proteins to migrate to the inner nuclear membrane (Braunagel et al., 1996). Proteins forming VLPs in *V.*
210 *canescens* could thus follow the same pathways as their homologous proteins in baculoviruses, nudiviruses,
211 hytrosaviruses, and bracoviruses due to the conservation of this mechanism among these viruses belonging
212 to the order Lefavirales (Braunagel et al., 1996; Hong et al., 1997; Braunagel et al., 2004; Abd-Alla et al.,
213 2008; Bézier et al., 2009; Braunagel et al., 2009).

214 **Phylogeny of Leptopilina venom and Venturia calyx RhoGAPs**

215 Searches for *N. vitripennis* RhoGAP sequences were performed using BLASTP at NCBI
216 (http://www.ncbi.nlm.nih.gov/blast/) and hmmsearch from the HMMER package (Eddy 2009) with the
217 RhoGAP (PF00620) HMM profile on the *N. vitripennis* v1.2 proteome database (Rago et al., 2016).
218 Multiple amino acid sequence alignments were performed using MAFFT with the --auto option (Katoh
219 and Standley 2013). For codon-based analysis of selection (see below), codon-based alignments of
220 complete coding sequences were performed using RevTrans
221 (https://services.healthtech.dtu.dk/service.php?RevTrans) with the amino acid alignments as templates.
222 Poorly aligned regions were removed using trimAl with the -automated1 option (Capella-Gutierrez et al.,
223 2009). Phylogenetic analyses were performed using maximum likelihood (ML) with IQ-TREE (Minh et al.,
224 2020). ModelFinder was used to select the best model selection for phylogeny (Kalyaanamoorthy et al.,
225 2017).

226 **Codon-based analysis of selection**

227 Codon-based alignments of complete coding sequences were performed with RevTrans using the
228 amino acid alignments as templates (see above). Phylogenetic analyses were performed using maximum
229 likelihood (ML) with PhyML (Guindon et al., 2010). Smart Model Selection was used to choose the best
230 model selection for the phylogeny (Lefort et al., 2017).
231 To detect evolutionary selective pressures acting on RhoGAP sequences, the ratios of non-synonymous
232 substitutions (dN) to synonymous substitutions (dS) were compared using different ML frameworks: the
233 CODEML program in the PAML (Phylogenetic Analysis by Maximum Likelihood) package (Yang 1997; Yang
234 2007), the HyPhy software implemented at http://www.datamonkey.org/ (Delport et al., 2010), and the
235 Selecton server (Stern et al., 2007) available at http://selecton.tau.ac.il/index.html.
236 Five different methods were used to detect codons under positive selection. In the first, codon
237 substitution models implemented in CodeML were applied to the codon-based alignment using the F3x4
238 frequency model. Two pairs of site models were used to determine whether some codons were under
239 positive selection: M1a (neutral) versus M2a (selection) and M7 (ß) versus M8 (ß & ω). The models were
240 compared using a likelihood ratio test (LRT) with 2 degrees of freedom to assess the significance of
241 detection of selection (Yang et al., 2000). Bayes Empirical Bayes (BEB) inference was then used to identify
242 amino acid sites with a posterior probability >95% of being under positive selection (Yang et al., 2005). We
243 then applied four other methods of detection of selection available in the HyPhy package: Single Likelihood
244 Ancestor Counting (SLAC), Fixed Effect Likelihood (FEL), Mixed Effects Model of Evolution (MEME) and Fast
245 Unbiased Bayesian AppRoximation (FUBAR) methods (Kosakovsky Pond & Frost 2005; Murrell et al., 2012;

246 Murrell et al., 2013). To eliminate false-positive detection, only codons identified by CodeML M2a and M8
247 and at least one of the other methods were considered under positive selection. Radical or conservative
248 replacements were then determined based on whether they involved a change in the physicochemical
249 properties of a given amino acid, such as charge or polarity (Zhang 2000).
250 Four different methods were used to detect codons under negative selection: the Selecton server using
251 the pair of site models M8a (ß& ω=1) versus M8 (ß& ω), and the FEL, SLAC and FUBAR methods mentioned
252 above. Only codons identified by Selecton and at least one other method were considered under purifying
253 selection.
254 To identify specific lineages with a proportion of sites evolving under positive or purifying selection, we
255 performed branch-site REL analyses using the HyPhy package (Kosakovsky Pond et al., 2011). Unlike the
256 branch and branch-site lineage-specific models available in CodeML, branch-site REL does not require *a*
257 *priori* identification of foreground and background branches.

258 **Structural analysis**
259 Molecular modeling of VcVLP2 RhoGAP was performed using the Phyre server with default parameters
260 (http://www.sbg.bio.ic.ac.uk/phyre2/) (Kelley et al., 2015). The model with the highest confidence (100%)
261 and coverage (46%) was obtained using the crystal structure with PDB code 2OVJ as a template. Model
262 quality was evaluated using the QMEAN server (http://swissmodel.expasy.org/qmean/) (Benkert et al.,
263 2011). Briefly, the QMEAN score is a global reliability score with values ranging between 0 (lower accuracy)
264 and 1 (higher accuracy). The associated Z-score relates this QMEAN score to the scores of a non-redundant
265 set of high-resolution X-ray structures of similar size, with ideal values close to 0. Visualization of LbGAP
266 (Colinet et al., 2007) and VcVLP2 structures and mapping of sites under selection were performed using
267 PyMol (http://sourceforge.net/projects/pymol/). Secondary structure assignment was performed with the
268 DSSP program (Kabsch & Sander 1983). Accessible surface area (ASA) or solvent accessibility of amino acids
269 was predicted using the *ASAView* algorithm (Ahmad et al., 2004).

270 ***In vitro* mutagenesis**
271 The S76K, V124K, L137D, T143L, S150L, I185K, E200G, and V203R mutations were introduced into the
272 LbGAP cDNA using the QuickChange XL Site-Directed Mutagenesis Kit (Stratagene). The results of *in vitro*
273 mutagenesis were verified by sequencing.

274 **Yeast two-hybrid analysis**
275 Interactions between LbGAP and LbGAP mutants and mutated forms of *Drosophila* RhoA, Rac1, Rac2
276 and Cdc42 GTPases were individually examined by mating as previously described (Colinet et al., 2007).
277 The plasmids expressing the GTPase proteins were tested against the pGADT7-T control vector, which
278 encodes a fusion between the GAL4 activation domain and the SV40 large T-antigen. Reciprocally, plasmids
279 producing LbGAP and LbGAP mutants were tested against the pLex-Lamin control vector. Interactions
280 between LbGAP and the Rac1 and Rac2 GTPases were used as positive controls (Colinet et al., 2007).
281 Interactions were initially tested by spotting five-fold serial dilutions of cells on minimal medium lacking
282 histidine and supplemented with 3-amino-triazole at 0.5 mM to reduce the number of false positives. ß-
283 galactosidase activity was then detected on plates (Fromont-Racine et al., 1997).

284 **Purification of Leptopilina venosomes and mass spectrometry analysis**
285 Twenty-five Lbm, Lby and Lh female venom apparatus were dissected, and the reservoirs were
286 separated from the gland and opened to release the venom content in 25 µl of Ringer's solution
287 supplemented with a protease inhibitor cocktail (Sigma). The venom suspension was centrifuged at 500xg
288 for 5 min to remove the residual tissues, then centrifuged at 15,000xg for 10 min to separate the vesicular
289 fraction from the soluble venom proteins (supernatant fraction) (Wan et al., 2019). The vesicular fraction
290 was then washed twice by resuspension in 25 µl of Ringer's solution followed by centrifugation at 15,000xg
291 for 10 min. The two samples were mixed with 4x Laemmli buffer containing ß-mercaptoethanol (v/v) and
292 boiled for 5 min. Proteins were then separated on a 6–16% linear gradient SDS-PAGE and the gel was silver
293 stained as previously described (Colinet et al., 2013). Identification of proteins by nano-LC-tandem mass
294 spectrometry (MS/MS) was performed on bands excised from the gels as previously described (Colinet et
295 al., 2013). MS/MS data analysis was performed with Mascot software (http://www.matrixscience.com),

296 licensed in house using the full-length coding sequences of the *Leptopilina* venom RhoGAP sequences. Data
297 validation criteria were (i) one peptide with individual ion score greater than 50 or (ii) at least two peptides
298 of individual ion score greater than 20. The mascot score is calculated as -10Log (p). The calculated FDR
299 (based on an automated decoy database search) was less than 1%. The mass spectrometry proteomics
300 data have been deposited to the ProteomeXchange Consortium via the PRIDE (Perez-Riverol et al., 2022)
301 partner repository with the dataset identifier PXD041695.

302 **Results**

303 **Leptopilina venom RhoGAPs probably emerged in the ancestor of the genus**

304 In the Figitidae, venom RhoGAPs have only been described for *L. boulardi* and *L. heterotoma* (Labrosse
305 et al., 2005; Colinet et al., 2013). A search for candidate homologs was performed in the transcriptomes of
306 *L. victoriae* and *L. clavipes*, two other *Leptopilina* species, *Gasnaspis* sp. G1, another member of the family
307 Figitidae, and *Andricus quercuscalicis* and *Synergus umbraculus,* two gall wasp species representatives of
308 the superfamily Cynipoidea outside of Figitidae (separated by approximately 50 Mya (Peters et al., 2017)).
309 The putative venom RhoGAPs were identified based on the presence of a signal peptide at the N-terminus
310 of the protein, followed by a RhoGAP domain (Table 1). Two transcript sequences encoding RhoGAP
311 domain-containing proteins predicted to be secreted were found in *L. victoriae* (LvGAP1 and LvGAP2) and
312 one in *L. clavipes* (LcGAP1), whereas none were found for *Gasnaspis* sp. G1, *A. quercuscalicis* and *S.*
313 *umbraculus* (Table 1 and Figure 1A). Our results therefore suggest that venom RhoGAPs are specific to the
314 genus *Leptopilina* although further taxon sampling would be required to fully support this hypothesis.

315 **Leptopilina venom RhoGAPs likely evolved from a single imperfect duplication of RacGAP1**

316 A phylogenetic analysis was performed to learn more about the evolutionary history of *Leptopilina*
317 venom RhoGAPs. The phylogeny was constructed based on the amino acid sequence of the RhoGAP
318 domain of these venom proteins and that of the 19 classical RhoGAPs we identified from the predicted
319 proteome of the jewel wasp *Nasonia vitripennis* (Supplementary Table S2). Prior to analysis, the coding
320 sequence was completed for two Lbm (LbGAP1.3 and LbGAP5), one Lby (LbGAPy6) and all three Lh venom
321 RhoGAPs. Two of the *Leptopilina* venom RhoGAPs, namely LhGAP3 and LcGAP1, were predicted to contain
322 two RhoGAP domains instead of one. Therefore, these two domains were separated for the analysis. The
323 resulting phylogeny identified NvRacGAP1 as the closest RhoGAP from *N. vitripennis* to all *Leptopilina*
324 venom RhoGAPs with confident support values (Figure 1B). Accordingly, the RhoGAP domain found in all
325 *Leptopilina* venom RhoGAPs was predicted to belong to the MgcRacGAP subfamily typically found in
326 RacGAP1-related proteins (Table 1).

327 The RacGAP1 coding sequence of *L. boulardi, L. heterotoma, L. victoriae and L. clavipes* was obtained
328 either by cloning and sequencing or by searching genomic data, and its domain organization was compared
329 with that of venom RhoGAPs (Figure 1C, Table 1 and Supplementary Figure S2). *Leptopilina* RacGAP1 has a
330 typical domain organization consisting of a coiled-coil region and a C1 motif (protein kinase C-like zinc
331 finger motif, a ~ 50 amino-acid cysteine-rich domain involved in phorbol ester/diacylglycerol and Zn^{2+}
332 binding) followed by a RhoGAP domain (Tcherkezian & Lamarche-Vane 2007). A large part of the RacGAP1
333 sequence spanning the coiled-coil region and the C1 motif is replaced by the signal peptide in all *Leptopilina*
334 venom RhoGAPs (Figure 1C, Table 1 and Supplementary Figure S2). This suggests that a unique incomplete
335 duplication of the RacGAP1 gene occurred in the ancestor of the *Leptopilina* genus, resulting in a truncated
336 duplicate encoding a RhoGAP with an altered N-terminus.

337 To further investigate this duplication event and the possible origin of the signal peptide, the genomic
338 sequences of *L. boulardi*, *L. heterotoma* and *L. clavipes* venom RhoGAPs and RACGAP1 were obtained,
339 either by cloning and sequencing or by searching in genomic data, and compared (Supplementary Table
340 S2). The genomic sequence of *Leptopilina* RacGAP1 consists of 10 exons with a "CC region", "C1 motif" and
341 "RhoGAP domain" encoded by exons 2 and 3, exons 5 and 6 and exons 7 and 8, respectively. The RhoGAP
342 domain is also encoded by two exons for venom RhoGAPs. These two exons are preceded by one to three
343 exons, with the signal peptide encoded by the first exon for most of them. Sequence comparisons revealed
344 similarities between venom RhoGAPs and *Leptopilina* RacGAP1 only for the sequence spanning the two
345 exons encoding the RhoGAP domain and part of the following one. No significant similarities were found
346 for the preceding exons at either the nucleotide or amino acid level (Supplementary Figure S3). This

supports the hypothesis of a partial duplication of the RacGAP1 gene in the ancestor of the *Leptopilina* genus, resulting in the loss of the sequence spanning exons 1 to 6, followed by further duplication of the ancestrally duplicated gene during the diversification of the genus *Leptopilina*.

The two consecutive RhoGAP domains found in LhGAP3 were grouped together with confident support values in the phylogenies (Figure 1B and Supplementary Figure S2). This suggests that a partial tandem duplication spanning exons 2 and 3 has occurred for this *L. heterotoma* venom RhoGAP. In contrast, the two RhoGAP domains found in LcGAP1 did not group together (Figure 1B and Supplementary Figure S2). However, the genomic sequence of LcGAP1 was not complete and we could not find the region corresponding to the second RhoGAP domain in the *L. clavipes* genome (Supplementary Table S3). Therefore, it is unclear whether the LcGAP1 coding sequence found in the transcriptome assembly is true or artifactual.

Table 1. Motif and domain organization of *Leptopilina* venom RhoGAPs. The signal peptide was predicted using SignalP at CBS. The RhoGAP domain (PF00620) and the RacGAP1 domain (PTHR46199) were identified using InterProScan. Two successive RhoGAP domains were found in LhGAP3 and LcGAP1. Lbm: *L. boulardi* ISm ; Lby: *L. boulardi* ISy ; Lh: *L. heterotoma* ; Lc: *L. clavipes* ; Lv: *L. victoriae.*

			Signal peptide		RhoGAP domain (PF00620)				RacGAP1 domain (PTHR46199)			
		Total length	From	To	From	To	Length	E-value	From	To	Length	E-value
Lbm	LbGAP	282	1	20	52	193	142	2.9e-32	38	267	230	7.0e-37
	LbGAP1.1	292	1	23	58	205	148	1.0e-19	42	255	214	7.0e-30
	LbGAP1.2	280	1	23	58	205	148	1.1e-19	42	255	214	1.3e-29
	LbGAP1.3	287	1	23	58	205	148	7.2e-17	42	253	212	1.3e-27
	LbGAP2.1	251	1	23	44	183	140	9.9e-26	26	234	209	5.5e-37
	LbGAP2.2	263	1	23	56	196	141	6.6e-26	49	246	198	1.3e-34
	LbGAP3	295	1	23	56	175	120	3.2e-12	42	266	225	1.2e-27
	LbGAP4	246	1	20	42	178	137	9.1e-11	38	218	181	5.6e-18
	LbGAP5	275	1	20	60	207	148	6.3e-23	41	251	211	2.4e-33
Lby	LbGAPy	286	1	20	52	193	142	1.6e-32	38	267	230	3.4e-37
	LbGAPy1.1	287	1	23	58	205	148	5.6e-17	42	255	214	9.9e-28
	LbGAPy1.2	325	1	23	56	203	148	2.9e-17	42	293	252	1.7e-26
	LbGAPy2	256	1	23	44	185	142	8.3e-27	26	234	209	1.5e-37
	LbGAPy3.1	281	1	23	56	175	120	1.8e-11	42	237	196	1.5e-25
	LbGAPy3.2	266	1	23	41	160	120	5.8e-12	28	222	195	6.4e-25
	LbGAPy4	274	1	20	42	177	136	7.4e-09	30	218	189	2.1e-17
	LbGAPy5	275	1	23	60	207	148	4.4e-24	41	251	211	1.2e-35
	LbGAPy6	239	1	20	53	194	142	8.2e-25	49	231	183	9.4e-34
Lh	LhGAP1	293	1	20	43	180	138	5.5e-36	41	289	249	1.0e-38
	LhGAP2	336	1	20	43	181	139	1.5e-29	45	275	231	8.2e-31
	LhGAP3	467	1	20	35	174	140	1.4e-22	34	221	188	1.3e-38
					257	396	140	2.2e-17				
Lc	LcGAP1	497	1	20	43	184	142	3.2e-30				
					249	384	136	3.5e-28	247	478	232	8.46e-71
Lv	LvGAP1	370	1	20	38	179	142	2.4e-30				
	LvGAP2	266	1	20	38	181	144	8.5e-23	33	224	192	3.7e-28

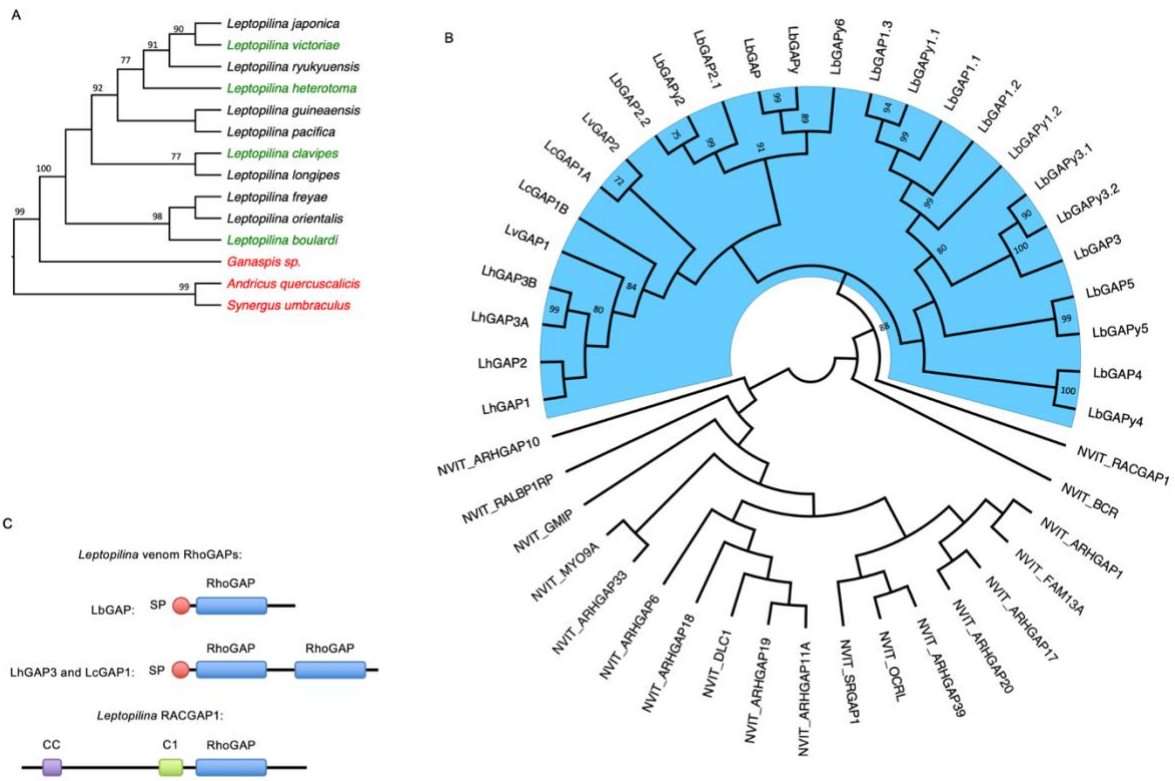

Figure 1. Origin of *Leptopilina* venom RhoGAPs (A) Maximum-likelihood phylogenetic tree of selected members of the Cynipoidea superfamily. The phylogenetic tree was obtained with IQ-TREE using internal transcribed spacer 2 (ITS2) sequence and displayed as a cladogram. Species in red are those for which venom RhoGAPs were not found. No data were available for species in black. (B) Maximum-likelihood phylogenetic tree of *Leptopilina* venom RhoGAPs along with *N. vitripennis* classical RhoGAPs. The phylogenetic tree was obtained with IQ-TREE using the RhoGAP domain amino acid sequence and displayed as a cladogram. For A and B, numbers at corresponding nodes are bootstrap support values in percent (500 bootstrap replicates). Only bootstrap values greater than 70% are shown. *Leptopilina* venom RhoGAPs are highlighted in blue. (C) Comparison of protein domain organization between LbGAP, representative of most *Leptopilina* venom RhoGAPs, LhGAP3 and LcGAP1, the two venom RhoGAPs that contain two RhoGAP domains, and *Leptopilina* RacGAP1. C1: protein kinase C-like zinc finger motif, CC: coiled-coil region, MgcRacGAP: RhoGAP domain found in RacGAP1-related proteins, SP: signal peptide.

L. boulardi and *L. heterotoma* venom RhoGAPs are associated with venosomes

LbGAP and LbGAP2 have been shown to be associated with vesicles named venosomes produced in *L. boulardi* venom that transport them to *Drosophila* lamellocytes (Wan et al., 2019). Our next goal was to investigate whether *Leptopilina* venom RhoGAPs other than LbGAP and LbGAP2 could be associated with venosomes. Proteomic analysis was performed on the supernatant and vesicular fractions separated from the venom by centrifugation. Comparison of the electrophoretic profiles obtained on a 6-16% SDS-PAGE for *L. boulardi* ISm (Lbm), *L. boulardi* ISy (Lby) and *L. heterotoma* (Lh) revealed an important variation between both fractions for all three wasps (Figure 2). All the major bands on the electrophoretic patterns of Lbm, Lby and Lh supernatant and vesicular fractions, as well as several minor bands (35 bands in total for Lbm, 34 for Lby and 37 for Lh), were excised and tryptic peptides were analyzed by mass spectrometry. The coding sequences of *Leptopilina* venom RhoGAPs were used to perform Mascot searches on the mass spectrometry data obtained from both venom fractions. All *L. boulardi* and *L. heterotoma* venom RhoGAPs were detected in the vesicular fraction, where most of them were found to be enriched (Figure 2). We

could then hypothesize that they are associated with and transported by venosomes to target *Drosophila* cells.

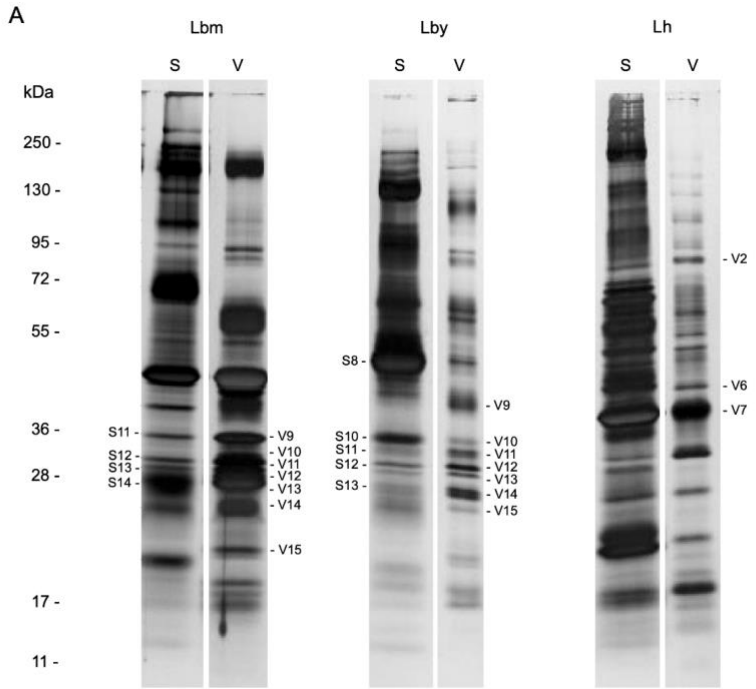

B

				Supernatant		Vesicular	
		Length	Predicted Mw	Protein band	Mascot Matches	Protein band	Mascot Matches
Lbm	LbGAP	282	32.13	**S11**/S12	11	**V9**/V10/V11/V12/ V13/V14/V15	57
	LbGAP1.1	292	33.02	S11/**S12**/S14	14	V9/**V10**/V11/V12/ V14/V15	85
	LbGAP1.2	280	31.99	S13	3	**V10**/**V11**/V12/V13	36
	LbGAP1.3	287	32.80	S12/**S13**/S14	12	V9/V10/**V11**/V12/ V13/V14/V15	85
	LbGAP2.1	251	28.81	S11/S12/S13/**S14**	14	V10/V11/V12/ **V13**/V14/V15	60
	LbGAP2.2	263	30.18	S12/S13/**S14**	9	V9/V10/V11/**V12**/ V13/V14/V15	85
	LbGAP3	295	34.01	**S12**/S13	3	**V10**/V11/V12/V13	15
	LbGAP4	246	28.57			V13/**V14**	3
	LbGAP5	275	31.72			**V10**/V11	10
Lby	LbGAPy	286	32.56	**S8**	1	**V10**/V11	4
	LbGAPy1.1	287	32.81	S10/S11/**S12**/S13	19	V11/**V12**/V13	19
	LbGAPy1.2	325	37.47			**V13**	1
	LbGAPy2	256	29.37	**S8**/S13	8	V12/V13/**V14**	8
	LbGAPy3.1	281	32.58	**S11**	1	V10/**V11**/V12/V13	5
	LbGAPy3.2	266	30.74	**S11**	1	V10/**V11**/V12/V13	5
	LbGAPy4	274	31.92	S10/**S11**/S12/S13	9	V9/V10/**V11**/V12/ V13/V14/V15	36
	LbGAPy5	275	32.04			**V12**	1
	LbGAPy6	239	27.83			**V15**	3
Lh	LhGAP1	293	33.16			**V7**	13
	LhGAP2	336	38.23			**V6**	4
	LhGAP3	467	53.92			**V2**	7

Figure 2. Proteomic analysis of *Leptopilina* venom supernatant and vesicular fractions. (A) The supernatant (S) and vesicular (V) fractions obtained from 25 Lbm, Lby and Lh venom reservoirs were separated on a 6-16% SDS-PAGE under reducing conditions and visualized by silver staining. Protein bands in which *Leptopilina* venom RhoGAPs were identified by mass spectrometry are numbered on the gel. Molecular weight standard positions are indicated on the left (kDa). (B) For each *Leptopilina* venom RhoGAP, length (number of amino acids), predicted Mw (kDa), bands in which specific peptides were found by mass spectrometry and number of total Mascot matches according to the S and V venom fractions are given. Numbers in bold correspond to the bands in which each RhoGAP was identified as the most abundant according to the number of Mascot matches.

403 ***V. canescens* calyx RhoGAPs probably evolved from two or more imperfect RacGAP1 duplication events**

404 Analysis of the *V. canescens* calyx transcriptome allowed the identification of a total of 13 RhoGAP
405 domain-containing protein coding sequences, including VcVLP2 (Table 2). Matches with peptides obtained
406 from a proteomic analysis of *V. canescens* VLPs (Pichon et al., 2015) were detected for all 13 calyx RhoGAPs,
407 indicating that they are associated with VLPs (Table 2).

408 Similar to the *Leptopilina* venom RhoGAPs, the *V. canescens* calyx RhoGAPs contain a MgcRacGAP1
409 domain (Table 2) and are closely related to NvRacGAP1 (Figure 3A). In contrast to the *Leptopilina* venom
410 RhoGAPs, none of the *V. canescens* calyx proteins were predicted to be secreted. Most were predicted to
411 be localized in the nucleus and/or to contain a nuclear localization signal (Supplementary Tables S4 and
412 S5). The absence of a predicted nuclear localization signal for VcGAP7 may be explained by the incomplete
413 coding sequence at the 5' end (Table 2). There is greater variation in domain organization for *V. canescens*
414 calyx RhoGAPs compared to *Leptopilina* venom RhoGAPs (Figure 3B and Supplementary Figure S4). Eight
415 *V. canescens* calyx RhoGAPs have retained the C1 motif. In addition, VcGAP12 still contains a CC region in
416 the N-terminal part of the sequence although the total sequence length is shorter than RacGAP1 (Figure
417 3B and Supplementary Figure S4).

418 **Table 2.** Motif and domain organization of *Venturia* calyx RhoGAP proteins associated with VLPs. The
419 coiled-coil (CC) region was predicted using COILS (Lucas et al., 1991). The protein kinase C-like zinc
420 finger (C1) motif (PS50081), the RhoGAP domain (PF00620) and the RacGAP1 domain (PTHR46199)
421 were identified using InterProScan. Mascot 5: number of matches with peptides from purified *V.*
422 *canescens* VLPs. [a]Coding sequence not complete at 5' end. [b]Coding sequence not complete at 3' end.

			CC		C1 (PS50081)		RhoGAP domain (PF00620)				RacGAP1 domain (PTHR46199)			
	Mascot	Total length	From	To	From	To	From	To	Length	E-value	From	To	Length	E-value
VcVLP2	26	485			56	106	134	277	144	7.4e-36	28	366	339	3.1e-98
VcGAP1	9	207					30	168	139	5.7e-25	12	199	188	5.1e-49
VcGAP2	19	280					23	161	139	6.9e-29	8	195	188	1.5e-50
VcGAP3	4	270			22	69	92	231	140	2.6e-25	14	265	252	2.9e-63
VcGAP4	21	382			37	86	116	240	125	2.2e-16	20	298	279	2.7e-68
VcGAP5	19	307			15	63	91	236	146	4.0e-24	7	281	275	2.6e-60
VcGAP6	16	284			17	67	88	215	128	3.3e-19	14	270	257	8.0e-55
VcGAP7	14	225[a]					15	156	142	5.3e-29	4	212	209	9.2e-57
VcGAP8	5	369			64	113	141	281	141	4.6e-28	20	334	315	3.6e-84
VcGAP9	9	319[b]			54	104	123	266	144	1.1e-28	38	306	269	5.5e-73
VcGAP10	5	233					30	166	137	1.6e-22	7	219	213	7.1e-45
VcGAP11	5	199					27	166	140	4.3e-19	8	198	191	5.7e-42
VcGAP12	8	402	21	48	79	131	159	296	138	3.3e-35	54	372	319	9.7e-91

423

424 The genomic coding sequence of VcRacGAP1 was obtained by genomic data mining. It comprised 9
425 exons with the CC region, C1 motif and RhoGAP domain encoded by exons 2 and 3, exons 5 and 6 and exon
426 7, respectively (Supplementary Table S6). In contrast to *Leptopilina*, the RhoGAP domain is encoded by a
427 single exon in *V. canescens* RacGAP1 as well as in all calyx RhoGAPs. Interestingly, the VcGAP12 gene is
428 located close to the VcRacGAP1 gene on chromosome 3, but is three exons shorter, suggesting a recent
429 incomplete duplication (Supplementary Table S6). In contrast, VcVLP2 and the other VcGAP genes are more
430 widely distributed in the *V. canescens* genome (Supplementary Table S6). It is therefore possible that
431 incomplete duplication events of the VcRacGAP1 gene, followed by further tandem and dispersed

duplication of the ancestrally duplicated genes, led to the current number of calyx RhoGAPs in *V. canescens* organized in several clusters comprising 2 or more genes in tandem arrays (Figure 3C).

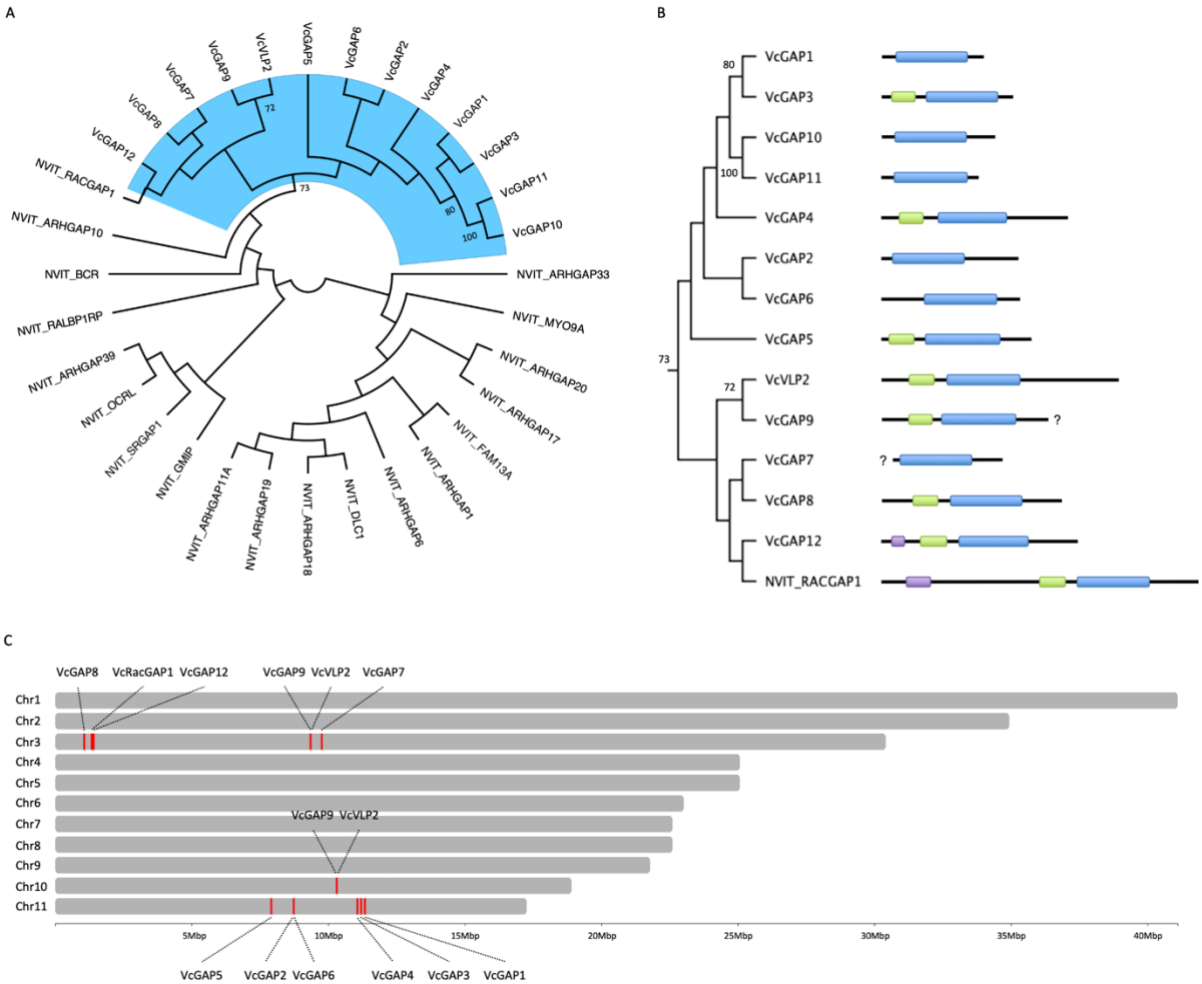

Figure 3. Origin of *V. canescens* calyx RhoGAPs (A) Maximum-likelihood phylogenetic tree of *V. canescens* calyx RhoGAPs along with *N. vitripennis* classical RhoGAPs. The phylogenetic tree was obtained with IQ-TREE using the RhoGAP domain amino acid sequence and displayed as a cladogram. Numbers at corresponding nodes are bootstrap support values in percent (500 bootstrap replicates). Only bootstrap values greater than 70% are shown. *V. canescens* calyx RhoGAPs are highlighted in blue. (B) Comparison of protein domain organization between *V. canescens* calyx RhoGAPs and *N. vitripennis* RacGAP1 using the RhoGAP domain as reference. The color code is as follows: purple for the coiled-coil region (CC), green for the protein kinase C-like zinc finger motif (C1) and blue for the RhoGAP domain. A (?) indicates that either the N- or C-terminal part of the sequence is unknown. (C) *V. canescens* chromosome map with the position of gene loci corresponding to RacGAP1 and calyx RhoGAPs visualized using chromoMap R package (Anand & Rodriguez Lopez 2022).

448 **Evidence of positive selection in *L. boulardi* venom and *V. canescens* calyx RhoGAP sequences**

449 In a previous work, we identified four amino acid residues involved in the interaction of LbGAP with
450 Rho GTPases (Colinet et al., 2007), including the key arginine residue (R74 in LbGAP) required for the GAP
451 catalytic activity (Figure 4A). The other 8 venom RhoGAP sequences found in *L. boulardi* Ism and ISy were
452 all mutated at this arginine residue (Figure 4B). Most also contained mutations in one or more of the other
453 three amino acids involved in Rho GTPase interaction (Figure 4B). Similarly, all *V. canescens* calyx RhoGAP
454 sequences, except VcVLP2, are mutated in one or more of the sites essential for GAP activity and/or
455 involved in the interaction with Rho GTPases (Figure 4C). These observations suggest that only LbGAP and
456 its homolog LbGAPy in *L. boulardi* and VcVLP2 in *V. canescens* are functional as RhoGAPs.

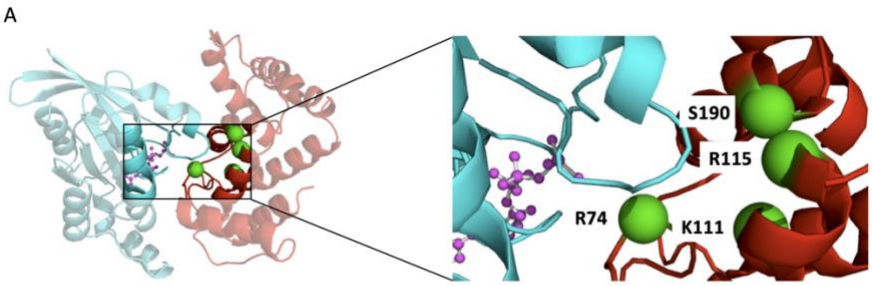

B

		74	111	115	190
	RacGAP1	R	K	R	T
Lbm	LbGAP	R	K	R	S
	LbGAP1.1	L	L	S	T
	LbGAP1.2	L	L	S	I
	LbGAP1.3	L	L	S	T
	LbGAP2.1	M	K	R	T
	LbGAP2.2	M	K	R	T
	LbGAP3	T	T	R	V
	LbGAP4	L	V	K	N
	LbGAP5	L	Q	Y	I
Lby	LbGAPy	R	K	R	S
	LbGAPy1.1	L	L	S	T
	LbGAPy1.2	S	I	S	T
	LbGAPy2	M	K	R	T
	LbGAPy3.1	T	T	R	V
	LbGAPy3.2	T	T	R	V
	LbGAPy4	L	V	K	N
	LbGAPy5	S	Q	Y	I
	LbGAPy6	F	K	R	T

C

		74	111	115	190
	RacGAP1	R	K	R	T
Vc	VLP2	R	K	R	T
	VcGAP1	G	K	A	I
	VcGAP2	Q	R	R	A
	VcGAP3	R	K	T	I
	VcGAP4	T	M	K	I
	VcGAP5	S	K	L	V
	VcGAP6	L	K	S	I
	VcGAP7	A	L	R	T
	VcGAP8	Q	K	R	V
	VcGAP9	K	K	R	V
	VcGAP10	R	K	S	I
	VcGAP11	T	K	F	I
	VcGAP12	R	K	A	T

457

458 **Figure 4. Mutations in the essential sites for GAP activity and/or involved in interaction with Rho**
459 **GTPases** (A) Tertiary structure of LbGAP (red) in complex with Rac1 (blue) and the transition-state
460 analogue GDP.AlF3 (modeled by homology for sequence spanning amino acid residues 51 to 216 in
461 Colinet et al., 2007). The four sites essential for GAP activity and/or involved in interaction with
462 RhoGTPases are colored green. (B) Amino acids found at the four sites essential for GAP activity
463 and/or involved in the interaction with RhoGTPases for *Leptopilina* RacGAP1 and *L. boulardi* venom
464 RhoGAP sequences. The numbering corresponds to the positions in the LbGAP sequence. (C) Amino
465 acids at the four sites essential for GAP activity and/or involved in interaction with RhoGTPases for
466 *V. canescens* RacGAP1 and calyx RhoGAP sequences. The numbering corresponds to the positions in
467 the LbGAP sequence. In B and C, amino acids are colored according to their properties following the
468 RasMol amino acid color scheme.

469 A search for positive selection was performed to detect possible functional divergence of *L. boulardi*
470 venom and *V. canescens* calyx RhoGAP sequences. PAML codon-based models with (M2a and M8) and
471 without (M1a and M7) selection were compared using likelihood ratio tests (LRTs). Both M1a/M2a and

472 M7/M8 comparisons resulted in the rejection of the null hypothesis suggesting that a fraction of codons in
473 RhoGAP sequences are under positive selection (Table 3).

474 **Table 3.** Positive selection analysis among sites using CodeML for *L. boulardi* venom and *V. canescens*
475 calyx RhoGAP sequences. lnL is the log likelihood of the model. p-value is the result of likelihood ratio
476 tests (LRTs). Global ω is the estimate of the dN/dS ratio under the model (given as a weighted
477 average). Parameters (ω > 1) are parameters estimates for a dN/dS ratio greater than 1.

478

L. boulardi

Model	lnL	p-value	Global ω	Parameters (ω > 1)
M1a: neutral	-5735.55		0.71	
M2a: selection	-5688.59	< 0.001	1.65	ω = 4.70, p = 0.21
M7: ß	-5741.07		0.70	
M8: ß&ω	-5688.19	< 0.001	1.56	ω = 4.4, p = 0.22

V. canescens

Model	lnL	p-value	Global ω	Parameters (ω > 1)
M1a: neutral	-12616.14		0.78	
M2a: selection	-12574.17	< 0.001	1.31	ω = 2.72, p = 0.28
M7: ß	-12612.64		0.73	
M8: ß&ω	-12564.70	< 0.001	1.21	ω = 2.30, p = 0.34

479

480 Consistently, a total of 7 and 11 branches of the phylogenetic tree constructed with the *L. boulardi*
481 venom and *V. canescens* calyx RhoGAP sequences, respectively, were detected by the REL branch-site test
482 as corresponding to lineages on which a subset of codons has evolved under positive selection (Figure 5A
483 and 6A). For *L. boulardi*, 6 of the 7 lineages under positive selection were internal branches, indicating that
484 selection occurred primarily before the separation of the *L. boulardi* Ism and ISy strains (Figure 5A).
485 The combined use of five different methods identified a total of 19 codons as candidates under positive
486 selection for the *L. boulardi* venom RhoGAP sequences, most of which were found in the region
487 corresponding to the RhoGAP domain (Figure 5B). In contrast, only 4 amino acids were detected as evolving
488 under negative selection in the *L. boulardi* venom RhoGAPs, respectively (Figure 5C). The leucine at position
489 9 in LbGAP is located in the signal peptide, demonstrating the importance of this region. The other three
490 amino acids in *L. boulardi* and most of those in *V. canescens* under negative selection are buried in the
491 protein and are probably important for the structural stability (Figures 5D and 5E).
492 Interestingly, at least one radical change in charge and/or polarity of the corresponding amino acids
493 was found for all selected codons (Figure 5B). For example, the polar uncharged serine residue at position
494 76 in LbGAP was replaced by a negatively charged lysine residue in LbGAP4 (Figure 5B). Since radical
495 changes are more likely to modify protein function than conservative changes, this suggests that the
496 identified non-synonymous substitutions may be adaptive. Interestingly, the corresponding amino acids
497 are mostly exposed on the surface of the protein and therefore likely to interact with partners (Figures 5C
498 and 5D).
499 We therefore generated site-specific mutants of LbGAP for 8 of the 19 amino acids under positive
500 selection and compared their binding capabilities to Rho GTPases. Two-hybrid analysis revealed a lack of
501 interaction for five of the mutants, indicating that the corresponding amino acids are essential for
502 interaction with Rac GTPases (Table 4). On the other hand, the remaining three mutants were still able to
503 interact strongly with Rac1 and Rac2, suggesting that the corresponding amino acids are not involved in
504 the interaction with Rac GTPases (Table 4).
505 For the *V. canescens* calyx RhoGAP sequences, six amino acids were identified as candidates under
506 positive selection and 19 under negative selection (Figures 6B and 6C). Four of the amino acids under
507 positive selection are predicted to be exposed on the surface of the protein, indicating functional
508 diversification in relation to interaction with partners as in *L. boulardi* (Figures 6D and 6E). Most of the
509 amino acids under negative selection are buried within the protein and are likely to be important for
510 structural stability (Figures 6D and 6E).

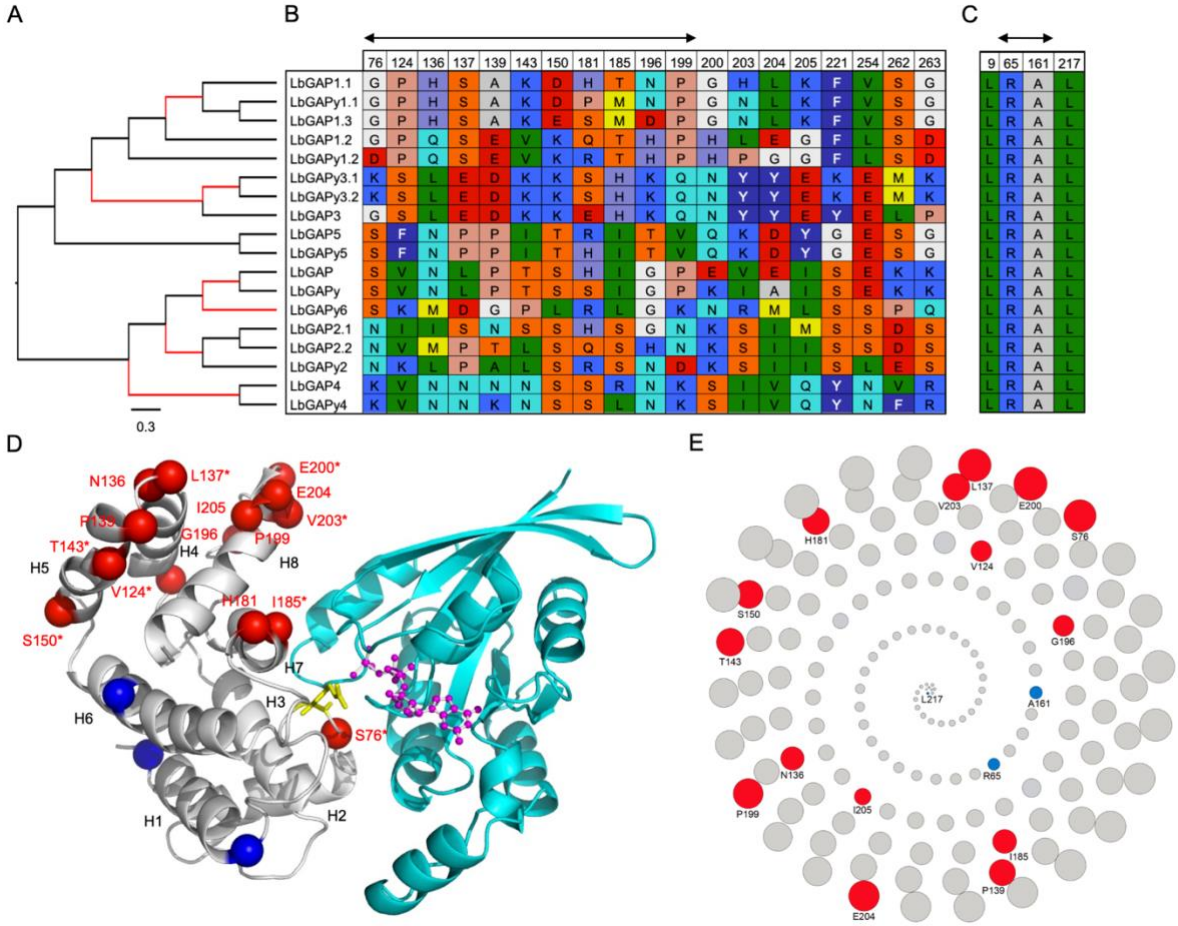

Figure 5. Identification of positively selected branches and codons in *L. boulardi* venom RhoGAPs. (A) Cladogram of *L. boulardi* venom RhoGAPs. Branches identified under positive selection by the HyPhy BSR method are colored in red. (B) Identified positively selected codons numbered according to LbGAP amino acid sequence. Amino acids are colored according to their properties following the RasMol amino acid color scheme. The two-sided arrow indicates sites located in the RhoGAP domain. (C) Identified negatively selected codons numbered according to LbGAP amino acid sequence. (D) Positively- and negatively selected sites displayed on the tertiary structure of LbGAP (grey) in complex with Rac1 (blue) and the transition-state analogue GDP.AlF3 (modeled by homology for sequence spanning amino acid residues 51 to 216 in Colinet et al., 2007). Helices are shown as ribbons and numbered according to their location in the amino-acid sequence of LbGAP. Positively selected sites are displayed as red-colored spheres and numbered according to the LbGAP sequence. A star indicates amino acid residues tested in mutagenesis and two-hybrid interaction assays. Negatively selected sites are displayed as spheres and colored in blue. Protruding LbGAP Arg74 is shown as sticks and colored in yellow. GDP.AlF3 is shown as ball-and-sticks models and colored in magenta. (E) Spiral view of LbGAP amino acids in the order of their solvent accessibility. Most accessible amino acids come on the outermost ring of the spiral whereas the buried amino acids are occurring in the innermost ring. Radius of the circles corresponds to the relative solvent accessibility. Red and blue colors are used for positively- and negatively selected amino acids respectively. All other amino acids are in grey.

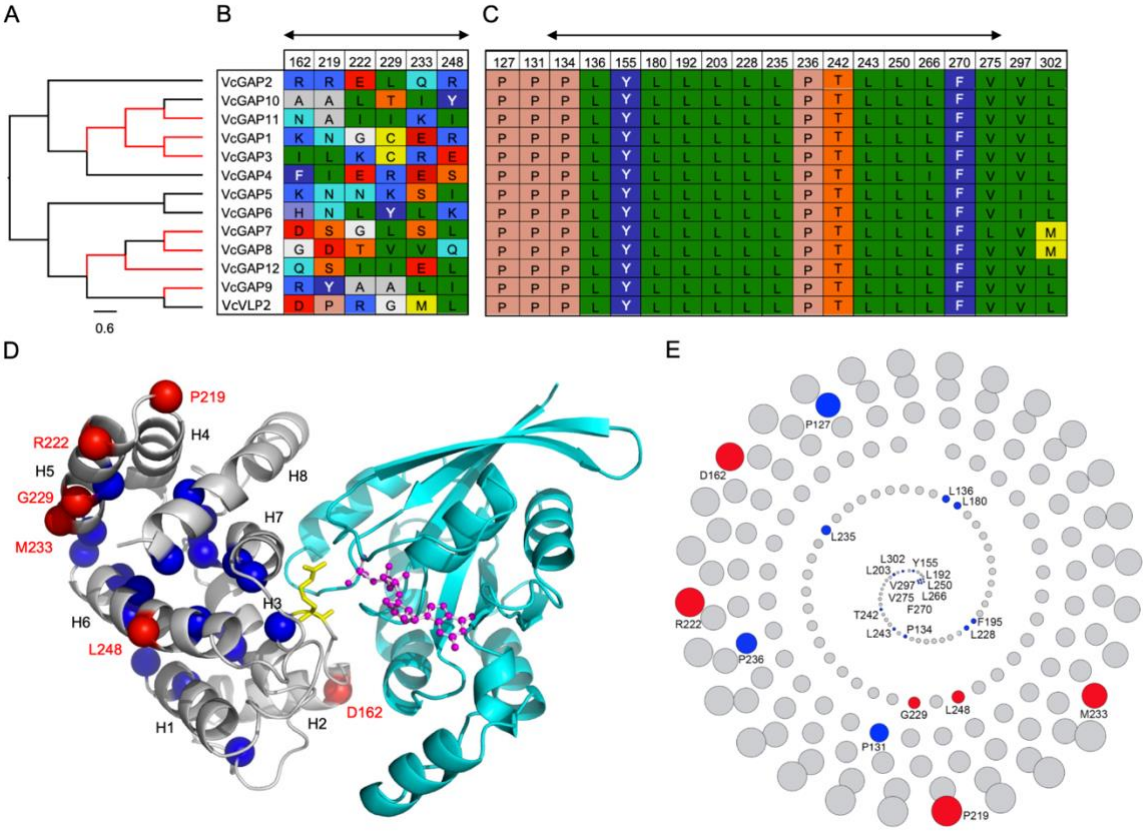

Figure 6. Identification of positively selected branches and codons in *V. canescens* calyx RhoGAPs. (A) Cladogram of *V. canescens* calyx RhoGAPs. Branches identified under positive selection by the HyPhy BSR method are colored in red. (B) Identified positively selected codons numbered according to VcVLP2 amino acid sequence. Amino acids are colored according to their properties following the RasMol amino acid color scheme. The two-sided arrow indicates sites located in the RhoGAP domain. (C) Identified negatively selected codons numbered according to VcvLP2 amino acid sequence. (D) Positively- and negatively selected sites displayed on the tertiary structure of VcVLP2 (grey) in complex with Rac1 (blue) and the transition-state analogue GDP.AlF3 (modeled by homology for sequence spanning amino acid residues 117 to 316). Helices are shown as ribbons and numbered according to their location in the amino-acid sequence of VcVLP2. Positively selected sites are displayed as red and negatively selected sites blue spheres, respectively, and numbered according to the VcVLP2 sequence. Protruding VcVLP2 Arg156 is shown as sticks and colored in yellow. GDP.AlF3 is shown as ball-and-sticks models and colored in magenta. (E) Spiral view of VcVLP2 amino acids in the order of their solvent accessibility. Most accessible amino acids come on the outermost ring of the spiral whereas the buried amino acids are occurring in the innermost ring. Radius of the circles corresponds to the relative solvent accessibility. Red and blue colors are used for positively- and negatively selected amino acids respectively. All other amino acids are in grey.

Table 4. Summary of the results of interaction assays for the LbGAP mutants. Results are based on growth on selective medium lacking histidine and qualitative ß-galactosidase overlay assays. -: no interaction; (+): very weak interaction; +++: strong interaction.

	LbGAP	LbGAP S76K	LbGAP V124K	LbGAP L137D	LbGAP T143L	LbGAP S150L	LbGAP I185K	LbGAP E200G	LbGAP V203R	T
Rac1	+++	-	-	+++	+++	+++	-	-	-	-
Rac2	+++	-	-	+++	+++	+++	-	-	-	-
CDC42	(+)	(+)	(+)	(+)	(+)	(+)	(+)	(+)	(+)	(+)
RhoA	-	-	-	-	-	-	-	-	-	-
Lamin	-	-	-	-	-	-	-	-	-	-

554 ## Discussion

555 **Independent convergent recruitment of vesicle-associated RhoGAP proteins in distantly related**
556 **parasitoid species**

557 The process of duplication of a gene encoding a protein usually involved in a key physiological process
558 whose function will be hijacked is a major mechanism of toxin recruitment (Fry et al., 2009; Wong & Belov
559 2012; Casewell et al., 2013). The results of phylogeny and domain analyses indicate that the *Leptopilina*
560 venom RhoGAPs and the calyx RhoGAPs found in *V. canescens* VLPs originated from duplication of the gene
561 encoding the cellular RacGAP1 in these species. This independent convergent recruitment may suggest a
562 similar function in virulence in these two evolutionarily distant parasitoid species. Consistently, our results
563 indicate that venom RhoGAPs in *L. boulardi* and *L. heterotoma* and calyx RhoGAPs in *V. canescens* are
564 associated with extracellular vesicles, named venosomes and VLPs, respectively. While these two types of
565 vesicles have different tissue origins and formation mechanisms, *Leptopilina* venosomes and *V. canescens*
566 VLPs would act as transport systems to deliver virulent proteins, including RhoGAPs, into host hemocytes
567 to alter their function (Pichon et al., 2015; Wan et al., 2019). However, the role of RhoGAPs on host
568 hemocytes is still unclear or even unknown, although we have previously shown that LbGAP inactivates
569 Rac-like GTPases (Colinet et al., 2007), which are required for successful encapsulation of *Leptopilina* eggs
570 (Williams et al., 2005; Williams et al., 2006).

571 RacGAP1 is an intracellular multidomain protein consisting of a coiled-coil region followed by a C1 motif
572 (protein kinase C-like zinc finger motif) and a RhoGAP domain (Tcherkezian & Lamane-Vane 2007).
573 *Leptopilina* venom RhoGAPs, on the other hand, possess only a RhoGAP domain preceded by a secretory
574 signal peptide. Sequence comparisons at the genomic level support the hypothesis of a single partial
575 duplication of the RacGAP1 gene in the ancestor of the *Leptopilina* genus, resulting in the loss of a 5' portion
576 of the sequence encoding the coiled-coil region and the C1 motif, followed by the acquisition of the signal
577 peptide sequence. This initial evolutionary event would then have been followed by further duplication of
578 the ancestral duplicate gene throughout the diversification of the genus *Leptopilina,* leading to the current
579 number of venom RhoGAPs. A first hypothesis for the origin of the signal peptide would be that the loss of
580 part of the 5' coding sequence in the duplicate resulted in a new N-terminal end for the encoded protein
581 with signal peptide properties. Modification of the N-terminal end of the protein into a fully functional
582 signal peptide may have required some point mutations after partial duplication, as in the case of the
583 antifreeze protein of an Antarctic zoarcid fish (Deng et al., 2010). Another possibility is that the signal
584 peptide originated from a process of partial duplication with recruitment (Katju & Lynch 2006), in which a
585 "proto-peptide signal" coding sequence was acquired from the new genomic environment into which the
586 partial copy was integrated. Finally, it is also possible that the new 5' region of the duplicated copy results
587 from a chimeric duplication (Katju & Lynch 2006), e.g. from the partial duplication of another gene or by
588 exon shuffling (Vibranovski et al., 2006). The acquisition of the signal peptide probably facilitated the
589 neofunctionalization of the venom RhoGAPs according to the evolutionary model of protein subcellular
590 relocalization (PSR) proposed by Byun McKay & Geeta (2007), according to which a modification of the N-
591 or C-terminal region of a protein can change its subcellular localization, by the loss or acquisition of a
592 specific localization signal, and enable it to acquire a new function.

593 In *V. canescens,* the N-terminal region of the calyx RhoGAPs is more variable in length, with some
594 proteins retaining the C1 motif upstream of the RhoGAP domain and one retaining a coiled-coil region
595 upstream of the C1 motif. Most of the *V. canescens* calyx RhoGAPs were predicted to contain a nuclear
596 localization signal, consistent with (i) the accumulation of VcVLP2 in the nucleus of the calyx cells prior to
597 its association with the virus-derived VLPs (Pichon et al., 2015) and (ii) our results from a proteomic analysis
598 indicating that all 13 calyx RhoGAPs are associated with VLPs. Human RacGAP1 has been described to
599 localize to the cytoplasm and nucleus (Mishima et al., 2002), suggesting that *V. canescens* calyx RhoGAPs
600 have retained the RacGAP1 nuclear localization signal, unlike *Leptopilina* venom RhoGAPs. One of the *V.*
601 *canescens* calyx RhoGAP genes is located close to the RacGAP1 gene in the genome, suggesting a recent
602 partial tandem duplication. The other genes, on the other hand, are scattered throughout the genome
603 suggesting that they originate from one or more older duplication events of the RacGAP1 gene. In contrast
604 to *Leptopilina*, it cannot be excluded that two or more partial duplication events of the RacGAP1-encoding
605 gene occurred in *V. canescens*, followed by further duplication of ancestral duplicates.

606 **Accelerated evolution through duplication and divergence: pseudogenization and/or**
607 **neofunctionalization?**
608 Our work revealed a significant divergence for the two multigene families of RhoGAPs in *L. boulardi*
609 and *V. canescens* compared to RacGAP1, illustrated by the presence of mutations on the arginine essential
610 for GAP activity and/or on one or more of the amino acids shown to be important, or even necessary, for
611 interaction with the Rac GTPases in all RhoGAPs except LbGAP (and its homolog LbGAPy) and VcVLP2. The
612 presence of mutations at key sites in the majority of *L. boulardi* venom and *V. canescens* calyx RhoGAPs
613 suggests a loss of function by pseudogenization. However, peptide matches were found in proteomic
614 analyses for each of these RhoGAPs, indicating that the corresponding genes are successfully transcribed
615 and translated. Furthermore, our results indicate that the ancestrally acquired secretory signal peptide, in
616 which we identified an amino acid under negative selection, is conserved in all *L. boulardi* RhoGAPs and
617 that most *V. canescens* RhoGAPs conserved the nuclear localization signal of RacGAP1. In addition, all
618 RhoGAPs retained the ability to associate with vesicles, namely venosomes in *L. boulardi* and VLPs in *V.*
619 *canescens*. Finally, we showed that several amino acids embedded in the protein structure evolved under
620 negative selection, suggesting that they are important for protein stability. Taken together, these
621 observations are not consistent with the hypothesis that any of the mutated RhoGAPs is undergoing a
622 pseudogenization process, although it cannot be excluded that this process is quite recent and could have
623 been initiated by the loss of the GAP active site.
624 An alternative hypothesis to pseudogenization would be functional diversification of the mutated
625 RhoGAPs independent of the Rho pathway. Indeed, we have evidenced an evolution under positive
626 selection for the majority of RhoGAPs in the two multigenic families. Most of the sites under positive
627 selection are located on the surface of the protein and are therefore likely to interact with partners. In
628 addition, directed mutagenesis and two-hybrid experiments in *L. boulardi* have shown that some of these
629 amino acids are not involved in the interaction with Rac GTPases. Although the majority of studies on the
630 RhoGAP domain concern the interaction with Rho GTPases, interactions with other proteins have also been
631 described (Ban et al., 2004; Xu et al., 2013), supporting the hypothesis of a neofunctionalization of the
632 mutated RhoGAPs. Further studies will be needed to determine which functions the mutated RhoGAPs
633 have acquired in relation to parasitism. Recently, a possible role has been proposed for one of the RhoGAPs
634 found in the venom of the ISy line of *L. boulardi* in the induction of reactive oxygen species (ROS) in the
635 central nervous system of *D. melanogaster* in the context of superparasitism avoidance (Chen et al., 2021).
636 However, ROS production is notably regulated by the GTPases Rac1 and Rac2 (Hobbs et al., 2014), whereas
637 this venom protein (named EsGAP1 in Chen et al., 2021 and corresponding to LbGAPy6 in our study) has
638 likely lost its RhoGAP activity due to a mutation on the arginine at position 74. Therefore, the mechanism
639 by which EsGAP1 would be involved in ROS induction is unclear.
640 Other potential viral factors involved in parasitic success have been described previously that are
641 encoded by large gene families and similarly correspond to truncated forms of cellular proteins that have
642 retained only a single conserved domain, such as protein tyrosine phosphatases (PTPs) or viral ankyrins (V-
643 ANKs) of bracoviruses. In the case of bracovirus PTPs, some are active as phosphatases, while others are
644 mutated in their catalytic site and have been shown to be inactive as PTPs (Provost et al., 2004). In the
645 latter case, as well as for V-ANK, it has been suggested that by binding to their target, they may act as
646 constitutive inhibitors of the function of the corresponding cellular protein (Provost et al., 2004;
647 Thoetkiattikul et al., 2005). Moreover, the model of adaptive evolution by competitive evolution of
648 duplicated gene copies (Francino 2005) predicts that after a first step in which different copies explore the
649 mutation space, once a protein with an optimal function is obtained, the other copies will begin to decay
650 and undergo pseudogenization. This can lead to intermediate situations where both functional and non-
651 functional proteins are produced, as observed for different virulence protein families of parasitoid wasps.
652 Some of the described features of *L. boulardi* and *V. canescens* RhoGAPs may suggest that a process of
653 competitive evolution is underway in *V. canescens* and *L. boulardi*, although our results are also consistent
654 with the hypothesis of a possible neofunctionalization of these vesicle-associated proteins as discussed
655 above.
656 In conclusion, we evidenced the independent convergent origin and accelerated evolution of a
657 multigene family of vesicle-associated RhoGAP proteins in two unrelated parasitic wasps. Strikingly, these
658 vesicles, which are similarly involved in parasitism, are produced in distinct organs: the venom apparatus
659 in *Leptopilina* and the ovarian calyx in *V. canescens*. In the case of *Leptopilina* RhoGAPs, the acquisition of

660 a secretory signal peptide after incomplete duplication of the RacGAP1 gene allowed secretion into the
661 venom where the vesicles are formed. *V. canescens* RhoGAPs, on the other hand, probably retained the
662 RacGAP1 nuclear localization signal, because it is in the nucleus of calyx cells that VLPs are formed. Another
663 striking point is that our results suggest a possible functional diversification of vesicle-associated RhoGAPs
664 in both species, with the exception of LbGAP in *L. boulardi* and VcVLP2 in *V. canescens*, which are probably
665 the only ones with RhoGAP activity. An open question would be whether all RhoGAPs are important for
666 parasite success, but by different mechanisms, independent of the Rho pathway or not, depending on
667 whether RhoGAPs are mutated or not.
668

669 **Acknowledgements**

670 We are highly grateful to Christian Rebuf for help in insects rearing. We also thank Pr. M. T. Kimura
671 (Hokkaido University, Japan) for providing biological material. We would also like to thank Anthony
672 Bretaudeau (INRIA, Rennes, France) for help in the use of the workflows available at the BIPAA platform,
673 the genotoul bioinformatics platform Toulouse Occitanie (Bioinfo Genotoul,
674 https://doi.org/10.15454/1.5572369328961167E12) for providing computing resources and the BIG
675 bioinformatics platform from the PlantBios infrastructure for providing facilities and technical support.

676 **Data and supplementary information availability**

677 Raw data from the Illumina RNASeq sequencing of the *L. victoriae* venom apparatus are available at
678 NCBI under the BioProject ID PRJNA974978.
679 The mass spectrometry proteomics data from *L. boulardi* and *L. heterotoma* venosomes have been
680 deposited to the ProteomeXchange Consortium via the PRIDE (Perez-Riverol et al., 2022) partner repository
681 with the dataset identifier PXD041695.
682 Supplementary information is available online at Data INRAE: https://doi.org/10.57745/K82IWQ

683 **Conflict of interest disclosure**

684 The authors declare that they comply with the PCI rule of having no financial conflicts of interest in
685 relation to the content of the article.
686 Jean-Luc Gatti and Marylène Poirié are recommenders of PCI Zoology.

687 **Funding**

688 This work was supported by the Department of Plant Health and Environment from INRAE and the
689 French Government (National Research Agency, ANR) through the "Investments for the Future" programs
690 LABEX SIGNALIFE ANR-11-LABX-0028-01 and IDEX UCAJedi ANR-15-IDEX-01.

691 **References**

692 Abd-Alla AM, Cousserans F, Parker AG, Jehle JA, Parker NJ, Vlak JM, Robinson AS, Bergoin M (2008) Genome
693 analysis of a *Glossina pallidipes* salivary gland hypertrophy virus reveals a novel, large, double-stranded
694 circular DNA virus. *Journal of Virology,* **82**, 4595-4611. https://doi.org/10.1128/jvi.02588-07
695 Anand L, Rodriguez Lopez CM (2022) ChromoMap: an R package for interactive visualization of multi-omics
696 data and annotation of chromosomes. *BMC Bioinformatics,* **23**, 33. https://doi.org/10.1186/s12859-
697 021-04556-z
698 Ban R, Irino Y, Fukami K, Tanaka H (2004) Human mitotic spindle-associated protein PRC1 inhibits
699 MgcRacGAP activity toward Cdc42 during the metaphase. *Journal of Biological Chemistry,* **279**, 16394-
700 16402. https://doi.org/10.1074/jbc.m313257200

701 Benkert P, Biasini M, Schwede T (2011) Toward the estimation of the absolute quality of individual protein
702 structure models. *Bioinformatics,* **27**, 343-350. https://doi.org/10.1093/bioinformatics/btq662
703 Bézier A, Herbinière J, Lanzrein B, Drezen JM (2009) Polydnavirus hidden face: the genes producing virus
704 particles of parasitic wasps. *Journal of Invertebrate Pathology,* **101**, 194-203.
705 https://doi.org/10.1016/j.jip.2009.04.006
706 Brameier M, Krings A, MacCallum RM (2007) NucPred--predicting nuclear localization of proteins.
707 *Bioinformatics,* **23**, 1159-1160. https://doi.org/10.1093/bioinformatics/btm066
708 Braunagel SC, Elton DM, Ma H, Summers MD (1996) Identification and analysis of an *Autographa californica*
709 nuclear polyhedrosis virus structural protein of the occlusion-derived virus envelope: ODV-E56.
710 *Virology,* **217**, 97-110. https://doi.org/10.1006/viro.1996.0097
711 Braunagel SC, Williamson ST, Saksena S, Zhong Z, Russell WK, Russell DH, Summers MD (2004) Trafficking
712 of ODV-E66 is mediated via a sorting motif and other viral proteins: facilitated trafficking to the inner
713 nuclear membrane. *Proceedings of the National Academy of Sciences,* **101**, 8372-8377.
714 https://doi.org/10.1073/pnas.0402727101
715 Braunagel SC, Cox V, Summers MD (2009) Baculovirus data suggest a common but multifaceted pathway
716 for sorting proteins to the inner nuclear membrane. *Journal of Virology,* **83**, 1280-1288.
717 https://doi.org/10.1128/jvi.01661-08
718 Byun McKay SA, Geeta R (2007) Protein subcellular relocalization: A new perspective on the origin of novel
719 genes. *Trends in Ecology & Evolution*, **22**, 338–344. https://doi.org/10.1016/j.tree.2007.05.002
720 Capella-Gutierrez S, Silla-Martinez JM, Gabaldon T (2009) trimAl: a tool for automated alignment trimming
721 in large-scale phylogenetic analyses. *Bioinformatics,* **25**, 1972-1973.
722 https://doi.org/10.1093/bioinformatics/btp348
723 Carton Y, Poirié M, Nappi AJ (2008) Insect immune resistance to parasitoids. *Insect Science,* **15**, 67-87.
724 https://doi.org/10.1111/j.1744-7917.2008.00188.x
725 Casewell NR, Wüster W, Vonk FJ, Harrison RA, Fry BG (2013) Complex cocktails: the evolutionary novelty
726 of venoms. *Trends in Ecology & Evolution,* **28**, 219-229. https://doi.org/10.1016/j.tree.2012.10.020
727 Chen S, Krinsky BH, Long M (2013) New genes as drivers of phenotypic evolution. *Nature Reviews Genetics,*
728 **14**, 645-660. https://doi.org/10.1038/nrg3521
729 Chen J, Fang G, Pang L, Sheng Y, Zhang Q, Zhou Y, Zhou S, Lu Y, Liu Z, Zhang Y, Li G, Shi M, Chen X, Zhan S,
730 Huang J (2021) Neofunctionalization of an ancient domain allows parasites to avoid intraspecific
731 competition by manipulating host behaviour. *Nature Communications,* **12**, 5489.
732 https://doi.org/10.1038/s41467-021-25727-9
733 Colinet D, Schmitz A, Depoix D, Crochard D, Poirié M (2007) Convergent use of RhoGAP toxins by eukaryotic
734 parasites and bacterial pathogens. PloS Pathog **3**: e203. https://doi.org/10.1371/journal.ppat.0030203
735 Colinet D, Schmitz A, Cazes D, Gatti J-L, and Poirié M (2010) The origin of intraspecific variation of virulence
736 in an eukaryotic immune suppressive parasite. *PLoS Pathogens,* **6**, e1001206.
737 https://doi.org/10.1371/journal.ppat.1001206
738 Colinet D, Deleury E, Anselme C, Cazes D, Poulain J, Azema-Dossat C, Belghazi M, Gatti J-L, Poirié M (2013)
739 Extensive inter- and intraspecific venom variation in closely related parasites targeting the same host:
740 the case of *Leptopilina* parasitoids of *Drosophila*. *Insect Biochemistry and Molecular Biology,* **43**, 601–
741 611. https://doi.org/10.1016/j.ibmb.2013.03.010
742 Deng C, Cheng C-HC, Ye H, He X, Chen L (2010) Evolution of an antifreeze protein by neofunctionalization
743 under escape from adaptive conflict. *Proceedings of the National Academy of Sciences,* **107**, 21593-
744 21598. https://doi.org/10.1073/pnas.1007883107
745 Delport W, Poon AF, Frost SD, Kosakovsky Pond SL (2010) Datamonkey 2010: A suite of phylogenetic
746 analysis tools for evolutionary biology. *Bioinformatics,* **26**, 2455-2477.
747 https://doi.org/10.1093/bioinformatics/btq429
748 Drezen J-M, Chevignon G, Louis F, Huguet E (2014) Origin and evolution of symbiotic viruses associated
749 with parasitoid wasps. *Current Opinion in Insect Science*, **6**, 35-43.
750 https://doi.org/10.1016/j.cois.2014.09.008
751 Du J, Lin Z, Volovych O, Lu Z, Zou Z (2020) A RhoGAP venom protein from *Microplitis mediator* suppresses
752 the cellular response of its host *Helicoverpa armigera*. *Developmental & Comparative Immunology,* **108**,
753 103675. https://doi.org/10.1016/j.dci.2020.103675

Dupas S, Frey F, Carton Y (1998) A single parasitoid segregating factor controls immune suppression in *Drosophila*. *Journal of Heredity,* **89**, 306-311. https://doi.org/10.1093/jhered/89.4.306

Edgar RC (2004) Muscle: multiple sequence alignment with high accuracy and high throughput. *Nucleic Acids Research,* **32**, 1792–1797. https://doi.org/10.1093/nar/gkh340

Eddy SR (2009) A new generation of homology search tools based on probabilistic inference. *Genome Informatics,* **23**, 205–211. https://doi.org/10.1142/9781848165632_0019

Feddersen I, Sander K, Schmidt O (1986) Virus-like particles with host protein-like antigenic determinants protect an insect parasitoid from encapsulation. *Experientia,* **42**, 1278-1281. https://doi.org/10.1007/BF01946422

Francino MP (2005) An adaptive radiation model for the origin of new gene functions. *Nature Genetics,* **37**, 573-577. https://doi.org/10.1038/ng1579

Fromont-Racine M, Rain JC, Legrain P (1997) Toward a functional analysis of the yeast genome through exhaustive two-hybrid screens. *Nature Genetics,* **16**, 277–282. https://doi.org/10.1038/ng0797-277

Fry BG, Roelants K, Champagne DE, Scheib H, Tyndall JDA, King GF, Nevalainen TJ, Normann JA, Lewis RJ, Norton RS, Renjifo D, Rodriguez de la Vega RC (2009) The toxicogenomic multiverse: convergent recruitment of proteins into animal venoms. *Annual Review of Genomics and Human Genetics,* **10**, 483–511. https://doi.org/10.1146/annurev.genom.9.081307.164356

Gatti J-L, Schmitz A, Colinet D, Poirié M (2012) Diversity of virus-like particles in parasitoids' venom: viral or cellular origin? In: Beckage NE, Drezen J-M, editors, Parasitoid viruses, pp. 181–192, London: Academic Press. https://doi.org/10.1016/B978-0-12-384858-1.00015-1

Godfray HCJ (1994) Parasitoids: behavioral and evolutionary ecology (Vol. 67): Princeton University Press. https://doi.org/10.2307/j.ctvs32rmp

Goecks J, Mortimer NT, Mobley JA, Bowersock GJ, Taylor J, Schlenke TA (2013) Integrative approach reveals composition of endoparasitoid wasp venoms. *PLoS One,* **8**, e64125. https://doi.org/10.1371/journal.pone.0064125

Goldberg T, Hecht M, Hamp T, Karl T, Yachdav G, Ahmed N, Altermann U, Angerer P, Ansorge S, Balasz K, Bernhofer M, Betz A, Cizmadija L, Do KT, Gerke J, Greil R, Joerdens V, Hastreiter M, Hembach K, Herzog M, Kalemanov M, Kluge M, Meier A, Nasir H, Neumaier U, Prade V, Reeb J, Sorokoumov A, Troshani I, Vorberg S, Waldraff S, Zierer J, Nielsen H, Rost B (2014) LocTree3 prediction of localization. *Nucleic Acids Research,* **42**, W350-355. https://doi.org/10.1093/nar/gku396

Guindon S, Dufayard JF, Lefort V, Anisimova M, Hordijk W, Gascuel O (2010) New algorithms and methods to estimate maximum-likelihood phylogenies: assessing the performance of PhyML 3.0. *Systematic Biology,* **59**, 307–321. https://doi.org/10.1093/sysbio/syq010

Haas BJ, Papanicolaou A, Yassour M, Grabherr M, Blood PD, Bowden J, Couger MB, Eccles D, Li B, Lieber M, MacManes MD, Ott M, Orvis J, Pochet N, Strozzi F, Weeks N, Westerman R, William T, Dewey CN, Henschel R, LeDuc RD, Friedman N, Regev A (2013) De novo transcript sequence reconstruction from RNA-seq using the Trinity platform for reference generation and analysis. *Nature Protocols,* **8**, 1494–1512. https://doi.org/10.1038/nprot.2013.084

Hobbs GA, Zhou B, Cox AD, Campbell SL (2014) Rho GTPases, oxidation, and cell redox control. *Small GTPases,* **5**, e28579. https://doi.org/10.4161/sgtp.28579

Hong T, Summers MD, Braunagel SC (1997) N-terminal sequences from *Autographa californica* nuclear polyhedrosis virus envelope proteins ODV-E66 and ODV-E25 are sufficient to direct reporter proteins to the nuclear envelope, intranuclear microvesicles and the envelope of occlusion derived virus. *Proceedings of the National Academy of Sciences,* **94**, 4050-4055. https://doi.org/10.1073/pnas.94.8.4050

Jancek S, Bézier A, Gayral P, Paillusson C, Kaiser L, Dupas S, Le Ru BP, Barbe V, Periquet G, Drezen J-M, Herniou E A (2013) Adaptive selection on bracovirus genomes drives the specialization of *Cotesia* parasitoid wasps. *PLoS One*, **8**, e64432. https://doi.org/10.1371/journal.pone.0064432

Jones P, Binns D, Chang H-Y, Fraser M, Li W, McAnulla C, McWilliam H, Maslen J, Mitchell A, Nuka G, Pesseat S, Quinn AF, Sangrador-Vegas A, Scheremetjew M, Yong S-Y, Lopez R, Hunter S (2014) InterProScan 5: genome-scale protein function classification. *Bioinformatics*, **30**, 1236–1240. https://doi.org/10.1093/bioinformatics/btu031

Kabsch W, Sander C (1983) Dictionary of protein secondary structure: pattern recognition of hydrogen-bonded and geometrical features. *Biopolymers,* **22**, 2577-2637. https://doi.org/10.1002/bip.360221211

Kalyaanamoorthy S, Minh BQ, Wong TKF, von Haeseler A, Jermiin LS (2017) ModelFinder: fast model selection for accurate phylogenetic estimates. *Nature Methods,* **14**, 587–589. https://doi.org/10.1038/nmeth.4285

Katju V, Lynch M (2006) On the formation of novel gene by duplication in the *Caenorhabditis elegans* genome. *Molecular Biology and Evolution,* **23**, 1056–1067. https://doi.org/10.1093/molbev/msj114

Katoh K, Standley DM (2013) MAFFT multiple sequence alignment software version 7: Improvements in performance and usability. *Molecular Biology and Evolution,* **30**, 772–780. https://doi.org/10.1093/molbev/mst010

Kelley LA, Mezulis S, Yates CM, Wass MN, Sternberg MJ (2015) The Phyre2 web portal for protein modeling, prediction and analysis. *Nature Protocols,* **10**, 845-858. https://doi.org/10.1038/nprot.2015.053

Kosakovsky Pond SL, Frost SD (2005) Not so different after all: a comparison of methods for detecting amino acid sites under selection. *Molecular Biology and Evolution,* **22**, 1208-1222. https://doi.org/10.1093/molbev/msi105

Kosakovsky Pond SL, Murrell B, Fourment M, Frost SD, Delport W, Scheffler K (2011) A random effects branch-site model for detecting episodic diversifying selection. *Molecular Biology and Evolution,* **28**, 3033-3043. https://doi.org/10.1093/molbev/msr125

Labrosse C, Stasiak K, Lesobre J, Grangeia A, Huguet E, Drezen J-M, Poirié M (2005) A RhoGAP protein as a main immune suppressive factor in the *Leptopilina boulardi* (Hymenoptera, Figitidae)-*Drosophila melanogaster* interaction. *Insect Biochemistry and Molecular Biology,* **35**, 93–103. https://doi.org/10.1016/j.ibmb.2004.10.004

Lefort V, Longueville J-E, Gascuel O (2017) SMS : Smart model selection in PhyML. *Molecular Biology and Evolution,* **34**, 2422-2424. https://doi.org/10.1093/molbev/msx149

Long M, VanKuren NW, Chen S, Vibranovski MD (2013) New gene evolution: little did we know. *Annual Review of Genetics,* **47**, 307-333. https://doi.org/10.1146/annurev-genet-111212-133301

Lucas A, Van Dyke M, Stock J (1991) Predicting coiled coils from protein sequences. *Science*, **252**, 1162-1164. https://doi.org/10.1126/science.252.5009.1162

Millar AH, Whelan J, Small I (2006) Recent surprises in protein targeting to mitochondria and plastids. *Current Opinion in Plant Biology,* **9**, 610-615. https://doi.org/10.1016/j.pbi.2006.09.002

Minh BQ, Schmidt HA, Chernomor O, Schrempf D, Woodhams MD, von Haeseler A, Lanfear R (2020) IQ-TREE 2: New models and efficient methods for phylogenetic inference in the genomic era. *Molecular Biology and Evolution,* **37**, 1530–1534. https://doi.org/10.1093/molbev/msaa015

Mishima M, Kaitna S, Glotzer M (2002) Central spindle assembly and cytokinesis require a kinesin-like protein/RhoGAP complex with microtubule bundling activity. *Developmental Cell,* **2**, 41–54. https://doi.org/10.1016/s1534-5807(01)00110-1

Mueller JC, Andreoli C, Prokisch H, Meitinger T (2004) Mechanisms for multiple intracellular localization of human mitochondrial proteins. *Mitochondrion,* **3**, 315-325. https://doi.org/10.1016/j.mito.2004.02.002

Murrell B, Wertheim JO, Moola S, Weighill T, Scheffler K, Kosakovsky Pond SL (2012) Detecting individual sites subject to episodic diversifying selection. *PLoS Genetics,* **8**, e1002764. https://doi.org/10.1371/journal.pgen.1002764

Murrell B, Moola S, Mabona A, Weighill T, Sheward D, Kosakovsky Pond SL, Scheffler K (2013) FUBAR: A fast, unconstrained bayesian approximation for inferring selection. *Molecular Biology and Evolution,* **30**, 1196-1205. https://doi.org/10.1093/molbev/mst030

Nakai K, Horton P (1999) PSORT: a program for detecting sorting signals in proteins and predicting their subcellular localization. *Trends in Biochemical Sciences,* **24**, 34-36. https://doi.org/10.1016/s0968-0004(98)01336-x

Novković B, Mitsui H, Suwito A, Kimura MT (2011) Taxonomy and phylogeny of *Leptopilina* species (Hymenoptera: Cynipoidea: Figitidae) attacking frugivorous drosophilid flies in Japan, with description of three new species. *Entomological Science,* **14**, 333–346. https://doi.org/10.1111/j.1479-8298.2011.00459.x

859 Pennacchio F, Strand MR (2006) Evolution of developmental strategies in parasitic Hymenoptera. *Annual*
860 *Review of Entomology,* **51**, 233–258. https://doi.org/10.1146/annurev.ento.51.110104.151029
861 Perez-Riverol Y, Bai J, Bandla C, Hewapathirana S, García-Seisdedos D, Kamatchinathan S, Kundu D, Prakash
862 A, Frericks-Zipper A, Eisenacher M, Walzer M, Wang S, Brazma A, Vizcaíno JA (2022). The PRIDE
863 database resources in 2022: A Hub for mass spectrometry-based proteomics evidences. *Nucleic Acids*
864 *Research,* **50**, D543-D552. https://doi.org/10.1093/nar/gkab1038
865 Peters RS, Krogmann L, Mayer C, Donath A, Gunkel S, Meusemann K, Kozlov A, Podsiadlowski L, Petersen
866 M, Lanfear R, Diez PA, Heraty J, Kjer KM, Klopfstein S, Meier R, Polidori C, Schmitt T, Liu S, Zhou X,
867 Wappler T, Rust J, Misof B, Niehuis O (2017) Evolutionary history of the Hymenoptera. *Current Biology,*
868 **27**, 1013-1018. https://doi.org/10.1016/j.cub.2017.01.027
869 Pichon A, Bézier A, Urbach S, Aury J-M, Jouan V, Ravallec M, Guy J, Cousserans F, Thézé J, Gauthier J,
870 Demettre E, Schmieder S, Wurmser F, Sibut V, Poirié M, Colinet D, da Silva C, Couloux A, Barbe V, Drezen
871 J-M, Volkoff A-N (2015) Recurrent DNA virus domestication leading to different parasite virulence
872 strategies. *Science Advances,* 1, e1501150. https://doi.org/10.1126/sciadv.1501150
873 Poirié M, Carton Y, Dubuffet A (2009) Virulence strategies in parasitoid Hymenoptera as an example of
874 adaptive diversity. *Comptes Rendus Biologies,* **332**, 311–320.
875 https://doi.org/10.1016/j.crvi.2008.09.004
876 Poirié M, Colinet D, Gatti J-L (2014) Insights into function and evolution of parasitoid wasp venoms. *Current*
877 *Opinion in Insect Science,* **6**, 52–60. https://doi.org/10.1016/j.cois.2014.10.004
878 Provost B, Varricchio P, Arana E, Espagne E, Falabella P, Huguet E, La Scaleia R, Cattolico L, Poirié M, Malva
879 C, Olszewski JA, Pennacchio F, Drezen JM (2004) Bracoviruses contain a large multigene family coding
880 for protein tyrosine phosphatases. *Journal of Virology,* **78**, 13090-13103.
881 https://doi.org/10.1128/jvi.78.23.13090-13103.2004
882 Rago, A, Gilbert DG, Choi J-H, Sackton TB, Wang X, Kelkar YD, Werren JH, Colbourne JK (2016) OGS2:
883 genome re-annotation of the jewel wasp *Nasonia vitripennis*. *BMC Genomics,* **17**, 678.
884 https://doi.org/10.1186/s12864-016-2886-9
885 Reineke A, Asgari S, Schmidt O (2006) Evolutionary origin of *Venturia canescens* virus-like particles. *Archives*
886 *of Insect Biochemistry and Physiology,* **61**, 123–133. https://doi.org/10.1002/arch.20113
887 Serbielle C, Chowdhury S, Pichon S, Dupas S, Lesobre J, Purisima E, Drezen J-M, Huguet E (2008) Viral
888 cystatin evolution and three-dimensional structure modelling: a case of directional selection acting on
889 a viral protein involved in a host-parasitoid interaction. *BMC Biology,* **6**, 38.
890 https://doi.org/10.1186/1741-7007-6-38
891 Serbielle C, Dupas S, Perdereau E, Héricourt F, Dupuy C, Huguet E, Drezen, J-M (2012) Evolutionary
892 mechanisms driving the evolution of a large polydnavirus gene family coding for protein tyrosine
893 phosphatases. *BMC Ecology and Evolution,* **12**, 253. https://doi.org/10.1186/1471-2148-12-253
894 Slater GSC, Birney E (2005) Automated generation of heuristics for biological sequence comparison. *BMC*
895 *Bioinformatics,* **6**, 31. https://doi.org/10.1186/1471-2105-6-31
896 Stern A, Doron-Faigenboim A, Erez E, Martz E, Bacharach E, Pupko T (2007) Selecton 2007: advanced
897 models for detecting positive and purifying selection using a Bayesian inference approach. *Nucleic Acids*
898 *Research,* **35**(Web Server issue), W506-511. https://doi.org/10.1093/nar/gkm382
899 Tcherkezian J, Lamarche-Vane N (2007). Current knowledge of the large RhoGAP family of proteins. *Biology*
900 *of the Cell,* **99**, 67–86. https://doi.org/10.1042/bc20060086
901 Thoetkiattikul H, Beck MH, Strand MR (2005) Inhibitor kappaB-like proteins from a polydnavirus inhibit NF-
902 kappaB activation and suppress the insect immune response. *Proceedings of the National Academy of*
903 *Sciences,* **102**, 11426-11431. https://doi.org/10.1073/pnas.0505240102
904 Vibranovski MD, Sakabe NJ, de Souza SJ (2006) A possible role of exon-shuffling in the evolution of signal
905 peptides of human proteins. *FEBS Letters,* **580**, 1621–1624.
906 https://doi.org/10.1016/j.febslet.2006.01.094
907 Wan B, Goguet E, Ravallec M, Pierre O, Lemauf S, Volkoff A-N, Gatti J-L, Poirié M (2019) Venom atypical
908 extracellular vesicles as interspecies vehicles of virulence factors involved in host specificity: the case
909 of a drosophila parasitoid wasp. *Frontiers in Immunology,* **10**, 1688.
910 https://doi.org/10.3389/fimmu.2019.01688
911 Williams MJ, Ando I, Hultmark D (2005) *Drosophila melanogaster* Rac2 is necessary for a proper cellular
912 immune response. *Genes to Cells*, **10**, 813–823. https://doi.org/10.1111/j.1365-2443.2005.00883.x

913 Williams MJ, Wiklund ML, Wikman S, Hultmark D (2006) Rac1 signalling in the *Drosophila* larval cellular
914 immune response. *Journal of Cell Science,* **119**, 2015–2024. https://doi.org/10.1242/jcs.02920
915 Wong ESW, Belov K (2012) Venom evolution through gene duplications. *Gene,* **13**, 59–69.
916 https://doi.org/10.1016/j.gene.2012.01.009
917 Xu J, Zhou X, Wang J, Li Z, Kong X, Qian J, Hu Y, Fang J-Y (2013) RhoGAPs attenuate cell proliferation by
918 direct interaction with p53 tetramerization domain. *Cell Reports,* **3**, 1526-1538.
919 https://doi.org/10.1016/j.celrep.2013.04.017
920 Yang Z (1997) PAML: a program package for phylogenetic analysis by maximum likelihood. *Bioinformatics,*
921 **13**, 555-556. https://doi.org/10.1093/bioinformatics/13.5.555
922 Yang Z (2007) PAML 4: phylogenetic analysis by maximum likelihood. *Molecular Biology and Evolution,* **24**,
923 1586-1591. https://doi.org/10.1093/molbev/msm088
924 Yang Z, Nielsen R, Goldman N, Pedersen AM (2000) Codon-substitution models for heterogeneous
925 selection pressure at amino acid sites. *Genetics,* **155**, 431-449.
926 https://doi.org/10.1093/genetics/155.1.431
927 Yang Z, Wong WS, Nielsen R (2005) Bayes empirical bayes inference of amino acid sites under positive
928 selection. *Molecular Biology and Evolution,* **22**, 1107–1118. https://doi.org/10.1093/molbev/msi097
929 Zhang J (2000) Rates of conservative and radical nonsynonymous nucleotide substitutions in mammalian
930 nuclear genes. *Journal of Molecular Evolution,* **50**, 56–68. https://doi.org/10.1007/s002399910007
931